Non-linear vibrations of free-edge thin spherical shells: modal interaction rules and 1:1:2 internal resonance

Oliver Thomas [a,*], C. Touzé [b], A. Chaigne [b]

[a] *Structural Mechanics and Coupled Systems Laboratory, CNAM, 2 rue Conté, 75003 Paris, France*
[b] *ENSTA-UME, Chemin de la Hunière, 91761 Palaiseau Cedex, France*

Abstract

This paper is devoted to the derivation and the analysis of vibrations of shallow spherical shell subjected to large amplitude transverse displacement. The analog for thin shallow shells of von Kármán's theory for large deflection of plates is used. The validity range of the approximations is assessed by comparing the analytical modal analysis with a numerical solution. The specific case of a free edge is considered. The governing partial differential equations are expanded onto the natural modes of vibration of the shell. The problem is replaced by an infinite set of coupled second-order differential equations with quadratic and cubic non-linear terms. Analytical expressions of the non-linear coefficients are derived and a number of them are found to vanish, as a consequence of the symmetry of revolution of the structure. Then, for all the possible internal resonances, a number of rules are deduced, thus predicting the activation of the energy exchanges between the involved modes. Finally, a specific mode coupling due to a 1:1:2 internal resonance between two companion modes and an axisymmetric mode is studied.

Keywords: Shallow spherical shells; Geometrical non-linearities; Internal resonances, Non-linear vibrations

1. Introduction

Structures with a thin geometry, like beams, arches, plates and shells, can exhibit large amplitude flexural vibrations, whose magnitude is comparable to the order of their thickness. In those cases, typical non-linear

behaviors can be observed, such as jump phenomena and energy exchanges between modal configurations and a linear prediction model is not sufficient (Nayfeh and Mook, 1979). In this paper, von Kármán non-linear dynamic equations are used in the special case of a shallow spherical cap in order to predict and simulate the observed phenomena.

In the literature devoted to geometrically non-linear (finite-amplitude) vibrations of shells, the largest part of the studies is concerned with circular cylindrical shells. The interested reader can refer to the exhaustive review proposed by (Amabili et al., 1998). For the case of spherical caps, most of the studies including geometrical non-linearities deal with axisymmetric deflections of perfectly symmetric structures. Moreover, the focus is generally put on dynamic buckling and snap-through behavior, whereas vibratory responses are seldom treated. Some works dealing with non-linear vibration of shells are briefly reviewed here and the interested reader can refer for a thorough bibliography to reviews of the literature by Leissa (1993b), Qatu (2002), Moussaoui and Benamar (2002) as well as the recent paper by Amabili and Païdoussis (2003). Evensen and Evan-Iwanowsky (1967) proposed a very complete work, analytical and experimental, and investigate buckling as well as non-linear vibrations of a clamped-edge spherical cap with the harmonic balance method. Gonçalves (1994) addressed the same problem, with geometrical imperfections, and used a Galerkin method with the analytical expressions of the mode shapes to solve the problem. Ye (1997) used a numerical Runge–Kutta method to solve the same problem. However, those studies are restricted to vibrations involving only one axisymmetric mode. A detailed study is proposed by Yasuda and Kushida (1984) who investigated the multi-mode axisymmetric response of a clamped spherical cap. The special case of a 1:2 internal resonance between two axisymmetric modes was addressed both theoretically and experimentally. Grossman et al. (1969) investigated the free oscillations axisymmetric frequencies dependence with the deflection amplitude, as a function of both the curvature of the shell and the boundary conditions. All those studies are restricted to axisymmetric vibrations. However, even if the excitation pattern is rotationally symmetric, a complete realistic study has to include asymmetric vibrations, since non-linear coupling between any modal configuration is likely to appear. Hui (1983) addressed one-mode asymmetric vibrations of a complete spherical shell with geometric imperfections and structural damping. To the knowledge of the authors, no analytical studies on non-linear multi-mode asymmetric vibrations of spherical shells have been published and the present work aims at filling this gap.

Spherical caps can be considered as a reference problem, mainly because their vibrations display important non-linear behaviors that are commonly observed in large deflection vibrations of thin structures. Firstly, as a consequence of the multiplicity of two of eigenfrequencies associated to asymmetric modes—a common feature of structures with an axisymmetric geometry (see e.g. Morand and Ohayon, 1995, Chapter 1)—1:1 internal resonances between companion modes are numerous and give rise to a variety of complex vibratory patterns, including traveling waves (see e.g. Tobias and Arnold, 1957; Raman and Mote, 2001; Touzé et al., 2002). Secondly, the curvature of the structure adds quadratic non-linearities in the oscillators that govern the dynamics of the system, whereas only cubic terms are present in the case of transversely symmetric structures such as rods and plates (Thomas et al., 2001). Thirdly, the spectral content of spherical shells depends on one geometrical parameter related to the curvature. Particular algebraic relations between natural frequencies can then be obtained for specific values of the curvature. As a consequence, numerous internal resonances that are related to both quadratic and cubic non-linear terms are likely to be observed on spherical shells. An example addressed in the present work is the 1:1:2 internal resonance between an axisymmetric mode and two companion modes.

The main goal of this paper is to present a exhaustive method for analysis and prediction of the large amplitude vibratory response of spherical shells, from the governing equations to their resolution. It extends a study on non-linear vibrations of circular plates (Touzé et al., 2002) to the case a curved shallow geometry. The non-linear behavior and the possible energy transfers between modal configurations related to the perfect axisymmetric geometry of the structure are especially addressed, extending results of the

literature. The free-edge boundary conditions have been chosen mainly because they are the easiest to realize experimentally. However, the results of the present study can be extended to any type of boundary conditions, provided they are in accordance with the rotational symmetry of the problem.

The non-linear partial differential equations (PDE) that govern the oscillations of the shell are expanded onto its eigenmodes. The main underlying assumptions of the model, as well as the hypothesis of shallowness, are discussed. Complete analytical expressions of the eigenmodes of the associated linear problem are derived and compared to a numerical solution. After expansion of the PDE onto the eigenmodes, a set of coupled second-order ordinary differential equations with quadratic and cubic non-linearities is obtained. The coefficients of the non-linear terms are calculated in the case of a perfect axisymmetric geometry and the coupling rules for the modal interactions are deduced. Possible truncation of the infinite dimensional problem are evaluated. Finally, the particular case of a 1:1:2 internal resonance is precisely investigated by a perturbation method, in the case of a harmonic forced excitation. The effect of slight imperfections of the structure is simulated by introducing slight differences in the companion modes frequencies. Experimental validations of the theoretical results will be presented in a forthcoming paper.

2. Formulation of the problem

2.1. Local equations

A spherical shell of thickness h, radius of curvature R and outer diameter $2a$, made of a homogeneous isotropic material of density ρ, Poisson's ratio ν and Young's modulus E, is considered. The geometry is specified in Fig. 1.

The equations of motions for shallow shells subjected to large deflections and moderate rotations, with small strain so that Hooke's law is verified, were derived by various authors in the case of particular geometries: Donnell (1934) and Evensen and Fulton (1965) for cylinders, Marguerre (1938), Leissa and Kadi (1971) and Alhazza (2002) for curved panels, Mushtari and Galimov (1961) and Koiter (1965) in the general case. A recent work presents a justification of these equations by an asymptotic method (Hamdouni and Millet, 2003). These equations have taken several names in the past: Donnell's equations, Marguerre's

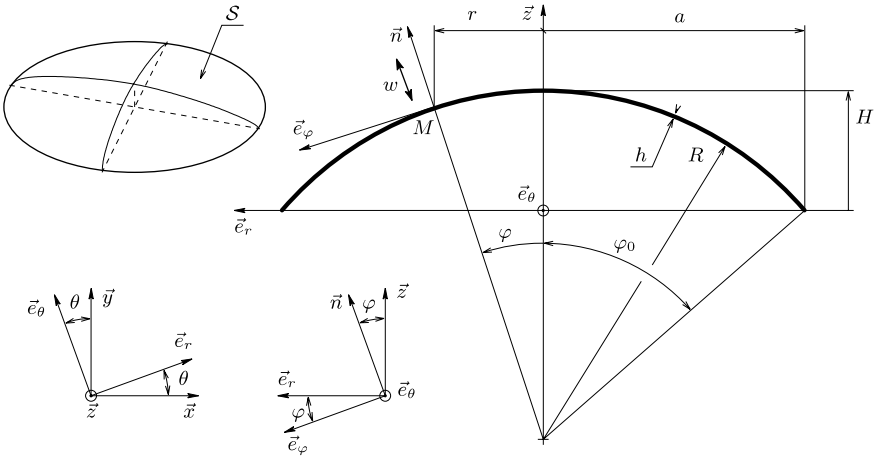


Fig. 1. Geometry of the shell: three-dimensional sketch and cross section.

equations, Koiter's equations or von Kármán's equations. They correspond to a generalization to the case of a curved geometry of von Kármán's model for large-deflection vibrations of plates (see e.g. Chu and Herrmann, 1956).

The main hypotheses are the following (see e.g. Koiter, 1965; Soedel, 1981):

- the shell is thin: $h/a \ll 1$ and $h/R \ll 1$;
- the shell is shallow: $a/R \ll 1$;
- the transverse normal stress are neglected with respect to the other stresses;
- Kirchhoff–Love hypotheses are used: the shear-strains are neglected and the normals to the undeformed mid-surface remain straight and normal and suffer no extension during the deformation;
- rotations of normals to the mid-surface are moderate, so that their sine and cosine are linearized (moderate rotations hypothesis);
- only the non-linear terms of the lowest order are kept in the strain expressions;
- the material is linear elastic, homogeneous and isotropic;
- in-plane and rotatory inertia are neglected;
- there is no membrane external forcing, which enables the use of an Airy stress function F.

With these assumptions fulfilled, one obtains the equations of motion in terms of the transverse displacement w along the normal to the mid-surface and the Airy stress function F, for all time t

$$D\Delta\Delta w + \frac{1}{R}\Delta F + \rho h\ddot{w} = L(w,F) - c\dot{w} + p, \tag{1a}$$

$$\Delta\Delta F - \frac{Eh}{R}\Delta w = -\frac{Eh}{2}L(w,w), \tag{1b}$$

where $D = Eh^3/12(1-\nu^2)$ is the flexural rigidity, c is a damping coefficient, p represents the external normal pressure, $\ddot{w}$ is the second partial derivative of w with respect to time, Δ is the Laplacian and L is a bilinear quadratic operator. With the assumption that the shell is shallow, angle φ defined in Fig. 1 is small and we get

$$\sin\varphi \simeq \varphi, \quad r = R\sin\varphi \simeq R\varphi. \tag{2}$$

Hence, the position of any point of the middle surface of the shell can be measured by its polar coordinates (r,θ), $r \in [0;a]$ and $\theta \in [0;2\pi]$ and the operators Δ and L of Eqs. (1a) and (1b) can be written

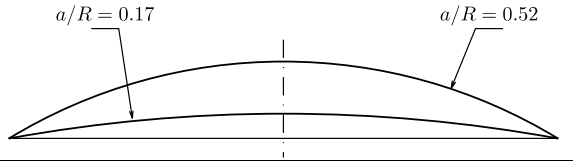
$$\Delta(\cdot) = (\cdot)_{,rr} + \frac{1}{r}(\cdot)_{,r} + \frac{1}{r^2}(\cdot)_{,\theta\theta} \tag{3}$$

and

$$L(w,F) = w_{,rr}\left(\frac{F_{,r}}{r} + \frac{F_{,\theta\theta}}{r^2}\right) + F_{,rr}\left(\frac{w_{,r}}{r} + \frac{w_{,\theta\theta}}{r^2}\right) - 2\left(\frac{w_{,r\theta}}{r} - \frac{w_{,\theta}}{r^2}\right)\left(\frac{F_{,r\theta}}{r} - \frac{F_{,\theta}}{r^2}\right), \tag{4}$$

where $(\cdot)_{,\alpha\beta} = \partial^2(\cdot)/\partial\alpha\partial\beta$. Expressions of F as a function of membrane stresses can be found in Touzé et al. (2002). Quadratic operator L defined by Eq. (4) has the same expression as in von Kármán's equations for circular plates (Efstathiades, 1971). A proof of Eqs. (1a) and (1b) can be obtained after writing the doubly curved panel equations formulated in Leissa and Kadi (1971) in polar coordinates.

The shallowness assumptions of Eq. (2) are valid as long as $\sin\varphi_0 \simeq \varphi_0$ (φ_0 is defined on Fig. 1). The corresponding shell geometries and limiting values of φ_0 are summarized in Fig. 2.



$\varphi_0/(\varphi_0^3/6) > 10$	$\varphi_0 > 31.4°$	$a/R < 0.52$	$H/a < 0.28$
$\varphi_0/(\varphi_0^3/6) > 100$	$\varphi_0 > 9.92°$	$a/R < 0.172$	$H/a < 0.087$

Fig. 2. Shell geometry so that Eqs. (2) are fulfilled, with $\sin\varphi_0 = a/R$. Parameters are defined on Fig. 1.

2.2. Free-edge boundary conditions

Boundary conditions are similar to those of a free-edge circular plate (Touzé et al., 2002) which yields for all t and θ

$$F \quad \text{and} \quad w \text{ are bounded at } r = 0, \tag{5a}$$

$$F_{,r} + \frac{1}{a}F_{,\theta\theta} = 0, \quad F_{,r\theta} - \frac{1}{a}F_{,\theta} = 0, \quad \text{at } r = a, \tag{5b}$$

$$w_{,rr} + \frac{\nu}{a}w_{,r} + \frac{\nu}{a^2}w_{,\theta\theta} = 0, \quad \text{at } r = a, \tag{5c}$$

$$w_{,rrr} + \frac{1}{a}w_{,rr} - \frac{1}{a^2}w_{,r} + \frac{2-\nu}{a^2}w_{,r\theta\theta} - \frac{3-\nu}{a^3}w_{,\theta\theta} = 0, \quad \text{at } r = a. \tag{5d}$$

The above equations stems from the vanishing of the external load at the edge: Eqs. (5b) are related to the membrane forces, Eq. (5c) to the bending moment and Eq. (5d) to the twisting moment and transverse shear force.

2.3. Dimensional analysis

Equations of motion (1a) and (1b) group different terms. On the one hand, terms ΔF in Eq. (1a) and Δw in Eq. (1b) are responsible for a *linear* coupling between transverse motion and membrane stretching, stemming from the curved geometry of the shell. On the other hand, terms $L(\cdot,\cdot)$ in both equations produce a *non-linear* coupling. Those two effects are independent from each other, since operator L is independent of curvature R. If R tends to infinity, one obtains von Kármán's equations (Efstathiades, 1971) for geometrically non-linear plates and if $L(\cdot,\cdot)$ vanishes, linear Donnell–Mushtari–Vlasov's model (Soedel, 1981) for shallow shells is obtained.

As the longitudinal inertia is neglected, F is slaved to transverse displacement w. Eq. (1b) shows that F contains both a linear and a quadratic term in w. By substituting F in Eq. (1a), one can show that curvature and non-linear coupling create together a *linear*, a *quadratic* and a *cubic* term in the equation that governs w, the first two terms arising from curvature. In order to balance their magnitude, dimensionless quantities (denoted by overbars) are introduced

$$w = w_0\bar{w}, \quad F = F_0\bar{F}, \quad r = a\bar{r}, \quad t = T_0\bar{t}, \quad \text{with } T_0 = a^2\sqrt{\frac{\rho h}{D}}. \tag{6}$$

w_0 and F_0 will be specified next. Substituting these variables in Eqs. (1a) and (1b) and omitting for clarity damping and forcing terms, one obtains for Eq. (1a)

$$\overline{\Delta\Delta w} + \ddot{\bar{w}} = -\chi\{\bar{w}\} + \frac{1}{2}\varepsilon_q\{\bar{w}^2\} - \varepsilon_c\{\bar{w}^3\}, \tag{7}$$

where $\{\bar{w}^n\}$ denotes a dimensionless term proportional to $\bar{w}^n$ supposed to be O(1). The order of magnitude of the different terms in Eq. (7) are specified by the following dimensionless factors:

$$\text{linear term } \{\bar{w}\}: \quad \chi = \frac{Eha^4}{DR^2} = 12(1-\nu^2)\frac{a^4}{R^2h^2}, \tag{8a}$$

$$\text{quadratic term } \{\bar{w}^2\}: \quad \varepsilon_q = \frac{Eha^2}{DR}w_0 = 12(1-\nu^2)\frac{a^2}{Rh^2}w_0, \tag{8b}$$

$$\text{cubic term } \{\bar{w}^3\}: \quad \varepsilon_c = \frac{Eh}{D}w_0^2 = 12(1-\nu^2)\frac{w_0^2}{h^2}. \tag{8c}$$

From these developments it appears naturally that curvature adds a linear term, which depends on the geometry of the shell only (parameter χ): it corresponds to the increase of transverse rigidity of the structure brought by the linear coupling between transverse motion and mid-plane stretching. It will be shown that χ brings a correction to the shell eigenfrequencies compared to those of the corresponding plate (Section 3.1).

Non-linear terms have the order of magnitude of ε_q and ε_c, which depends on the scaling w_0 of transverse displacement. As

$$\varepsilon_c = \varepsilon_q^2/\chi, \tag{9}$$

we find that cubic terms are of one order of magnitude smaller than that of quadratic terms. It is the usual scaling chosen for those terms when a perturbation method is used to solve the problem, so that these terms appear successively in the perturbative scheme (Nayfeh and Mook, 1979). We can also remark that the coefficient of cubic terms ε_c is independent of curvature R and that it is equal to the value it has in the case of a plate.

As a consequence, the balance between the magnitudes of the different terms is governed by the order of magnitude of transverse displacement w_0 only. Table 1 summarizes values obtained for ε_q and ε_c, for various choices of w_0 as compared to h. If the deflection is of the same order as the thickness (say $w_0 = h$), ε_q and ε_c are greater than 1, no small parameter appears in Eq. (7) and non-linear terms are of a larger order than linear terms. If the deflection is chosen one order smaller than h (i.e. $w_0 = h^2/a$), cubic terms only are small compared to the linear ones. This is the usual scaling chosen in the case of plate (Sridhar et al., 1978; Touzé et al., 2002). When curvature is non-negligible, one has to choose deflection two orders smaller than

Table 1
Analytical values and order of magnitude of ε_q and ε_c for various choice of transverse displacement scaling w_0 and shell geometries ($a/R = 0$ corresponds to a plate)

a/R	h/a	χ	$w_0 = h$		$w_0 = h^2/a$		$w_0 = h^3/a^2$	
			ε_q	ε_c	ε_q	ε_c	ε_q	ε_c
			$\frac{12(1-\nu^2)a^2}{Rh}$	$12(1-\nu^2)$	$\frac{12(1-\nu^2)a}{R}$	$\frac{12(1-\nu^2)h^2}{a^2}$	$\frac{12(1-\nu^2)h}{R}$	$\frac{12(1-\nu^2)h^4}{a^4}$
0	0.01	0	0	10	0	10^{-3}	0	10^{-7}
0	0.1	0	0	10	0	10^{-1}	0	10^{-3}
0.01	0.01	10	10	10	10^{-1}	10^{-3}	10^{-3}	10^{-7}
0.01	0.1	0.1	1	10	10^{-1}	10^{-1}	10^{-2}	10^{-3}
0.1	0.01	1000	10^2	10	1	10^{-3}	10^{-2}	10^{-7}
0.1	0.1	10	10	10	1	10^{-1}	10^{-1}	10^{-3}

χ, ε_q and ε_c are defined by Eqs. (8a)–(8c).

thickness ($w_0 = h^3/a^2$) to obtain both quadratic and cubic terms smaller than the linear ones. This is the solution adopted here since a perturbation method will be used in Section 5 to solve Eqs. (1a) and (1b). The above developments about scaling of the deflection w_0 show that non-linear phenomena become significant in curved structures for deflections of an order of magnitude between h^3/a^2 and h^2/a, smaller than in the case of plates.

The scaling F_0 of the stress function is chosen so that dimensionless variable F is O(1) when $\overline{\Delta\Delta F} \simeq -1/2\overline{L(w,w)}$ in Eq. (1b). This solution is suitable for any R, especially if R tends to infinity (the case of a plate). The following dimensionless variables are then defined:

$$r = a\bar{r}, \quad t = a^2\sqrt{\rho h/D}\bar{t}, \quad w = h^3/a^2\bar{w}, \quad F = Eh^7/a^4\bar{F}, \tag{10a}$$

$$c = [2Eh^4/Ra^2]\sqrt{\rho h/D}\bar{\mu}, \quad p = Eh^7/Ra^6\bar{p}. \tag{10b}$$

Substituting the above definitions in equations of motion (1a) and (1b) and dropping the overbars in the results, one obtains

$$\Delta\Delta w + \varepsilon_q \Delta F + \ddot{w} = \varepsilon_c L(w,F) + \varepsilon_q[-2\mu\dot{w} + p], \tag{11a}$$

$$\Delta\Delta F - \frac{a^4}{Rh^3}\Delta w = -\frac{1}{2}L(w,w), \tag{11b}$$

where $\varepsilon_q = 12(1-\nu^2)h/R$ and $\varepsilon_c = 12(1-\nu^2)h^4/a^4$. Boundary conditions (5a)–(5d), take the same form, with $a = 1$. Forcing and damping terms are scaled to the order of quadratic terms since only those nonlinear terms will be retained in the study of Section 5.

3. Modal analysis of the linear problem

3.1. Eigenfrequencies and mode shapes

An analytical expression of the natural frequencies of vibration of spherical shells with free-edge, axisymmetric as well as asymmetric, was proposed by Johnson and Reissner (1956). The main steps of the derivation of the expressions of the natural frequencies and mode shapes can be found in Appendix A and only some remarks are considered here.

The eigenmodes of the problem are the solutions of

$$\Delta\Delta\Phi + \chi\Delta\Psi - \omega^2\Phi = 0, \tag{12a}$$

$$\Delta\Delta\Psi = \Delta\Phi. \tag{12b}$$

They depend on one geometrical parameter only, the curvature parameter χ, that includes the joint influence of R, a and h. Transverse and membrane mode shapes $\Phi_{kn}(r,\theta)$ and $\Psi_{kn}(r,\theta)$ have k nodal diameters and n nodal circles. Associated dimensionless angular frequencies ω_{kn} are related to their dimensioned counterpart f_{kn} (in Hz) by the formula

$$f_{kn} = \frac{1}{2\pi a^2}\sqrt{\frac{D}{\rho h}}\omega_{kn} = \frac{h}{2\pi a^2}\sqrt{\frac{E}{12\rho(1-\nu^2)}}\omega_{kn}. \tag{13}$$

As membrane inertia is neglected, membrane motion is slaved to transverse motion. There are no membrane natural frequencies and each eigenfrequency ω_{kn} is associated to $\Phi_{kn}(r,\theta)$ and $\Psi_{kn}(r,\theta)$ (Kalnins, 1964).

The modes with at least one nodal diameter ($k \geqslant 1$) are called asymmetric modes. Each associated eigenfrequency has a multiplicity of two and the two corresponding independent modes are called *companion* or *preferential configurations*. The deformed shape of the first deduces from the other by a rotation of $\pi/2k$ around the symmetry axis.

3.2. Dependence on curvature

Fig. 3 shows the evolutions of several eigenfrequencies ω_{kn} with curvature parameter χ and suggests to classify the modes in two families.

- The first family groups all asymmetric modes $(k,0)$ with k nodal diameters ($k \geqslant 2$ since mode $(1,0)$ is a solid-body mode) and no nodal circles. These modes can be called *purely asymmetric*, and their natural frequencies only slightly depend on the curvature (Fig. 3). Their deformed shape is shown in Fig. 4 and their dependence on χ is shown on Fig. 5. Their transverse deformed shapes Φ only slightly depend on the curvature and on the contrary, membrane deformed shapes Ψ show a significant dependence on curvature.
- The second family groups axisymmetric modes $(0,n)$ with n nodal circles and asymmetric modes with at least one nodal circle (thus called *mixed* modes), since their frequencies increase with curvature and are always sorted in the same order (Fig. 3). Their deformed shape is shown in Fig. 6. For $k \in \{0,1\}$ the deformed shape do not depends on curvature (see Eq. (A.14) in Appendix A). For $k \geqslant 2$, the dependence is almost not visible (see Fig. 7), for both transverse and membrane modes.

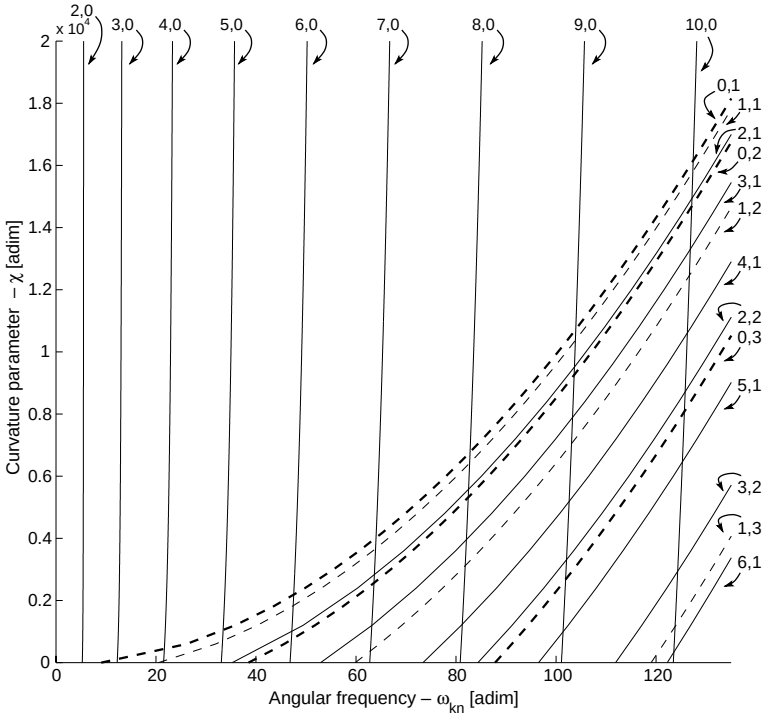


Fig. 3. Dimensionless natural frequencies ω_{kn} of the shell as a function of curvature parameter χ. (k,n) denotes the number of nodal diameters and circles, respectively.

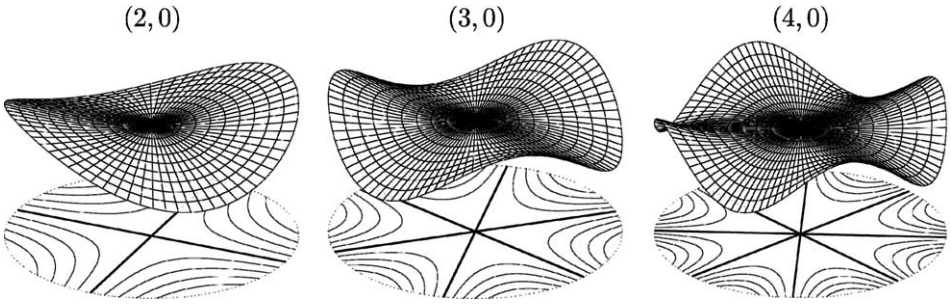


Fig. 4. First three asymmetric mode shapes $\Phi_{kn}(r,\theta)$ with no nodal circles, classified in ascending order of their frequencies.

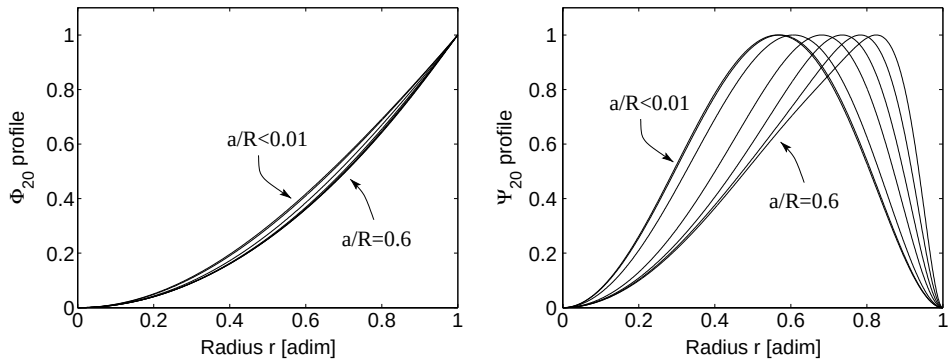


Fig. 5. Profiles of theoretical asymmetric $(2,0)$ mode shape, for several values of a/R between 0 and 0.6: (left) transverse mode and (right) membrane mode.

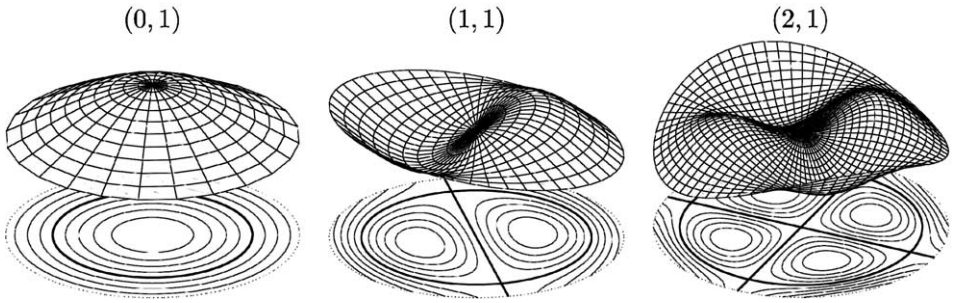


Fig. 6. First three axisymmetric and asymmetric mode shapes $\Phi_{kn}(r,\theta)$ with at least one nodal circle, classified in ascending order of their frequencies.

This analysis of the linear properties of the shell have importance even if one is interested in analyzing the non-linear vibratory regimes. The values of the natural frequencies governs the possible internal resonances relationships between modes and thus the possible modal interactions. This will be addressed in Section 4.2. The spatial dependence of the mode shapes are directly related to the values of the

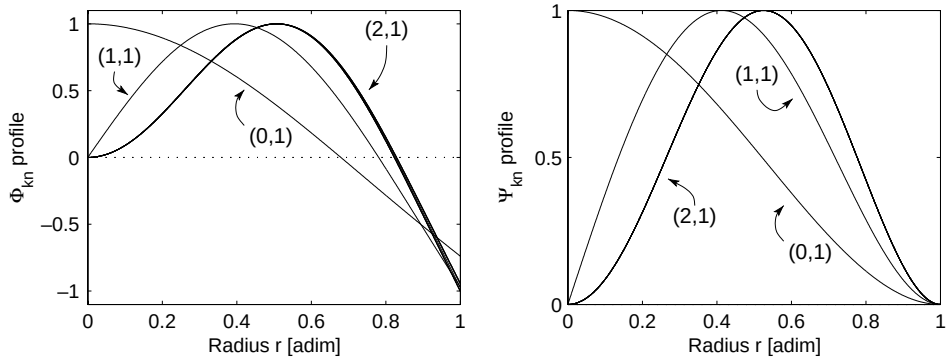


Fig. 7. Profiles of theoretical axisymmetric $(0,1)$ and asymmetric $(1,1)$ and $(2,1)$ mode shapes, for $a/R \in [0, 0.6]$: (left) transverse mode and (right) membrane mode.

coefficients of the non-linear terms that governs the exchanges of energy between modes. This will be addressed in Sections 4.3 and 4.4

3.3. Comparison with a numerical solution

In order to precise the validity range of the assumptions of shallowness of Eq. (2), theoretical results of Section 3.1 are compared to a numerical modal analysis, using the finite elements code CASTEM 2000 (Verpeaux et al., 1988) with DKT elements. Fig. 8 shows that the shallow theory predicts the natural frequencies with an error less than 1%, provided that $a/R < 0.3$. This result is in agreement with Table 2. A similar result has been established by Kalnins (1964) who compared the analytical natural frequencies stemming from (12a) and (12b) written in spherical coordinates—the so called non-shallow shell theory—to those of the shallow theory, derived by Johnson and Reissner (1956) and used in the present study.

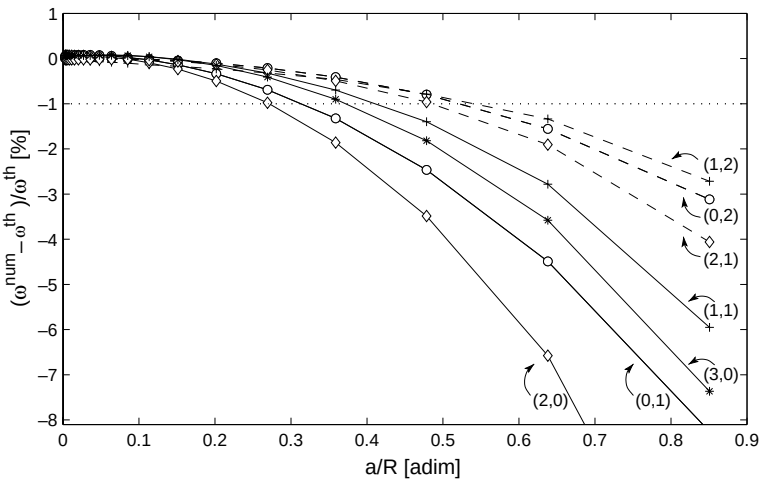


Fig. 8. Ratio of analytical ω^{th} and numerical ω^{num} solutions for the eigenfrequencies of the shell, in percent, as a function of a/R. Geometry of the simulated shell is defined by $a = 300\,\text{mm}$ and $h = 1\,\text{mm}$ and several values of R.

Table 2
Conditions on the number of nodal diameters and the expression in sine and cosine of the modes (both conditions must be fulfilled simultaneously) that lead to non-zero coefficients β^s_{pq} and Γ^s_{pqu}

$\beta^s_{pq} \neq 0$ $\Downarrow$ $k_s \in \{k_p + k_q, \mid k_p - k_q \mid\}$			$\Gamma^s_{pqu} \neq 0$ $\Downarrow$ $\{k_p + k_q, \mid k_p - k_q \mid\} \cap \{k_s + k_u, \mid k_s - k_u \mid\} \neq \emptyset$			
Φ_s	Φ_p	Φ_q	Φ_p	Φ_q	Φ_s	Φ_u
cos	cos	cos	cos	cos	cos	cos
	sin	sin	cos	cos	sin	sin
sin	cos	sin	sin	sin	cos	cos
	sin	cos	sin	sin	sin	sin
			cos	sin	cos	sin
			cos	sin	sin	cos
			sin	cos	sin	cos
			sin	cos	cos	sin

In order to study vibrations of shells with large curvature, it is possible to use in the following: (i) the eigenmodes calculated with a theoretical modal analysis in spherical coordinates (Kalnins, 1964), or (ii) to use numerical eigenmodes, calculated for example with the finite element method (see e.g. Lobitz et al., 1977, in the case of irregular plates). These tasks are beyond the scope of this article.

4. Modal expansion

4.1. Analytical expressions of the coupling coefficients

The aim of this section is to find a solution to the governing non-linear partial differential equations (11a) and (11b). The transverse deflection is expanded on the eigenmodes of the associated linear problem. The solution is sought as

$$w(r,\theta,t) = \sum_{p=1}^{+\infty} \Phi_p(r,\theta) q_p(t). \tag{14}$$

The $\{q_p\}_{p\in\mathbb{N}^*}$ are unknown functions of time—the modal coordinates—and Φ_p is the pth mode shape of the shell with free edge, whose analytical expression is given in Appendix A.

First, Eq. (11b) is solved by considering that

$$F = F_1 + F_2 \quad \text{with } \Delta\Delta F_1 = \frac{a^4}{Rh^3}\Delta w, \tag{15a}$$

$$\Delta\Delta F_2 = -\frac{1}{2} L(w,w). \tag{15b}$$

Eq. (15a) has already been solved for computing the linear modes in Section 3.1. Eq. (15b) shows the same form as for a circular plate ($\chi = 0$). It can be solved by using functions $\Upsilon_b(r,\theta)$ that exhibit the same spatial dependence as the transverse mode shapes of a clamped circular plate (Touzé et al., 2002). Their expression, along with the values of zeros ξ_b, can be found in Appendix B. Finally, the stress function is written

$$F(r,\theta,t) = F_1 + F_2 = \frac{a^4}{Rh^3}\left(\sum_{b=1}^{+\infty} \Psi_b(r,\theta) q_b(t) + \sum_{b=1}^{+\infty} \Upsilon_b(r,\theta) \sum_{p=1}^{+\infty}\sum_{q=1}^{+\infty} G^b_{pq} q_p(t) q_q(t)\right) \tag{16}$$

with

$$G^b_{pq} = -\frac{1}{2\xi_b^4}\iint_{\mathscr{S}_\perp} L(\Phi_p,\Phi_q)\Upsilon_b \mathrm{d}S \quad \text{and} \quad \iint_{\mathscr{S}_\perp} \Upsilon_b^2 \mathrm{d}S = 1, \tag{17}$$

where $\mathscr{S}_\perp$ is the projected surface $\mathscr{S}$ of the shell, i.e. the domain defined by $(r,\theta) \in [0 \quad 1] \times [0\ 2\pi]$.

This solution can now be substituted into (11a). Using Eq. (12a), multiplying by Φ_s, integrating over $\mathscr{S}_\perp$ and using the orthogonality properties of the modes leads to, for all $s \geqslant 1$

$$\ddot{q}_s(t) + \omega_s^2 q_s(t) = \varepsilon_{\mathrm{q}}\left[-\sum_{p=1}^{+\infty}\sum_{q=1}^{+\infty}\beta^s_{pq} q_p(t) q_{\mathrm{q}}(t) - 2\mu_s \dot{q}_s(t) + \tilde{Q}_s(t)\right] - \varepsilon_{\mathrm{c}}\sum_{p=1}^{+\infty}\sum_{q=1}^{+\infty}\sum_{r=1}^{+\infty}\Gamma^s_{pqr} q_p(t) q_{\mathrm{q}}(t) q_r(t), \tag{18}$$

where modal damping μ_s, depending on mode Φ_s, has been considered. Expressions of $\tilde{Q}_s(t)$, β^s_{pq} and Γ^s_{pqr} are

$$\tilde{Q}_s(t) = \iint_{\mathscr{S}_\perp} \Phi_s(r,\theta) p(r,\theta,t) \mathrm{d}S, \tag{19}$$

$$\beta^s_{pq} = -\iint_{\mathscr{S}_\perp} \Phi_s L(\Phi_p,\Psi_q)\mathrm{d}S - \frac{1}{2}\sum_{b=1}^{+\infty}\frac{1}{\xi_b^4}\iint_{\mathscr{S}_\perp} L(\Phi_p,\Phi_q)\Upsilon_b \mathrm{d}S \iint_{\mathscr{S}_\perp} \Phi_s \Delta\Upsilon_b \,\mathrm{d}S, \tag{20}$$

$$\Gamma^s_{pqu} = \frac{1}{2}\sum_{b=1}^{+\infty}\frac{1}{\xi_b^4}\iint_{\mathscr{S}_\perp} L(\Phi_p,\Phi_q)\Upsilon_b \,\mathrm{d}S \iint_{\mathscr{S}_\perp} \Phi_s L(\Phi_u,\Upsilon_b)\mathrm{d}S, \tag{21}$$

with, for all $p \geqslant 1$

$$\iint_{\mathscr{S}_\perp} \Phi_p^2 \mathrm{d}S = 1. \tag{22}$$

4.2. Reduced-order model

The initial problem described by the set of coupled partial differential equations (11a) and (11b) has been replaced by the *equivalent* discretized problem of the set (18) of non-linear coupled differential equations together with Eq. (14). At this stage, various approaches—analytical, numerical or a combination of both—can be used to solve the problem. In each cases, one has to truncate the set (18) to a finite number of oscillators. This operation has to be carefully performed, since a too crude truncation lead to predict erroneous results for the trend of non-linearity (see e.g. Nayfeh et al., 1992; Amabili et al., 1999; Touzé et al., 2004). The non-linear normal modes and the normal form theory offers a theoretical framework that allows to properly truncate the set (18) (see e.g. Touzé et al., 2004; Touzé and Thomas, 2004). In particular, it is shown that all the non-linear modes involved in internal resonances must be retained in the analysis. In our problem with quadratic and cubic non-linear terms, internal resonances are defined by the possible following relations between the natural frequencies of the shell:

$$\text{quadratic}: \quad \omega_p \simeq 2\omega_q \quad \text{or} \quad \omega_p \simeq \omega_{\mathrm{q}} \pm \omega_k, \tag{23a}$$

$$\text{cubic}: \quad \omega_p \simeq 3\omega_q \quad \text{or} \quad \omega_p \simeq 2\omega_q \pm \omega_k \quad \text{or} \quad \omega_p \simeq \omega_{\mathrm{q}} \pm \omega_k \pm \omega_m. \tag{23b}$$

4.3. Coupling rules

For a perfect axisymmetric structure, mode shapes with k nodal diameter are written in terms of $\cos k\theta$ and $\sin k\theta$. As coefficients β^s_{pq} and Γ^s_{pqu} involve integrations of products of those functions (see Eqs. (20) and (21)), a number of them vanish. The goal of the present section is to exhibit some rules that determine which coefficients vanish and consequently which modal interactions are possible. The mathematical derivations can be found in Appendix C.

Conditions for β^s_{pq} and Γ^s_{pqu} to be non-zero are summarized in Table 2. They depend on (i) the number of nodal diameters k_s, k_p, k_q and k_u of the modes Φ_s, Φ_p, Φ_q and Φ_u involved in the calculation of β^s_{pq} and Γ^s_{pqu} and (ii) the angular dependence in $\cos k\theta$ or $\sin k\theta$ of each of Φ_s, Φ_p, Φ_q and Φ_u. The number n of nodal circles has no influence.

Among those coefficients, some of them are involved in *resonant* non-linear terms. Those terms are called resonant because they can be viewed as forcing terms that excite a particular mode close to its resonance, when internal resonances relations between the natural frequencies exist. They are thus responsible for strong coupling—and thus large energy exchanges—between modal configurations. They cannot be removed by the computation of the normal form and thus govern the dynamics of the system (Guckenheimer and Holmes, 1983). As some coefficients vanish, the corresponding resonant terms are canceled and certain energy exchanges are impossible, even if relations of the form of Eqs. (23a) and (23b) are fulfilled. The end of this section exhibits a few rules that enable to predict the possible modal interactions.

In order to determinate if a particular modal interaction is possible, one has (i) to check if any of Eqs. (23a) and (23b) is fulfilled and (ii) to check if the associated resonant terms are non zero, using the following rules that hold on the number of nodal diameters of the involved modes. The rules holding on the nature in sine or cosine of companion modes are secondary because they cannot be responsible of cancellation of *all* resonant terms in a particular internal resonance. They are thus not addressed here.

The first rule stands that *all axisymmetric modes can be involved in modal interactions with one another, by both order-two* (Eq. (23a)) *and order three* (Eq. (23b)) *internal resonances*. Studies on modal interactions between axisymmetric modes were proposed by Sridhar et al. (1975) for circular plates and by Yasuda and Kushida (1984) in the case of spherical shells. The other rules, specifically related to particular internal resonances involving asymmetric modes, are given below. One should keep in mind that two asymmetric modes with natural frequencies such that $\omega_2 > \omega_1$ can have their numbers of nodal diameters such that $k_2 < k_1$: this situation exists if the numbers of nodal circles are such that $n_2 > n_1$ (see e.g. Fig. 3).

4.3.1. Order-two internal resonances

The coupling rules are summarized in Tables 3 and 4. Each table specifies the internal resonance considered (first line), the involved modes (second line), the resonant terms (third line) and the general conditions

Table 3
Rules determining if modal interaction between modes Φ_1 and Φ_2 is possible, when internal resonance $\omega_2 = 2\omega_1$ is fulfilled

$\omega_2 = 2\omega_1$		
Modes	Φ_1 (ω_1, k_1)	Φ_2 (ω_2, k_2)
Resonant terms	$q_1 q_2$	q_1^2
Rules	$k_1 \in \{k_1 + k_2, \lvert k_1 - k_2\rvert\} \neq \emptyset$	$k_2 \in \{2k_2, 0\} \neq \emptyset$
Nature of involved modes		Modal interaction
Both modes axisymmetric: $k_1 = k_2 = 0$		Possible
Only mode Φ_1 asymmetric: $k_1 \neq 0$, $k_2 = 0$		Possible $\forall k_1$
Only mode Φ_2 asymmetric: $k_1 = 0$, $k_2 \neq 0$		Impossible
Both modes asymmetric: $k_1 \neq 0$, $k_2 \neq 0$		Possible if $k_2 = 2k_1$

k_p is the number of nodal diameters of mode Φ_p, and q_p is the time evolution of mode Φ_p in set (18).

Table 4
Rules determining if modal interaction between modes Φ_1, Φ_2 and Φ_3 is possible, when internal resonance $\omega_3 = \omega_1 + \omega_2$ is fulfilled

$\omega_3 = \omega_1 + \omega_2$			
Modes	$\Phi_1(\omega_1, k_1)$	$\Phi_2\ (\omega_2, k_2)$	$\Phi_3(\omega_3, k_3)$
Res. terms	$q_2 q_3$	$q_1 q_3$	$q_1 q_2$
Rule	for all three res. terms: $k_1 \in \{k_2 + k_3, \lvert k_2 - k_3 \rvert\} \neq \emptyset$		

Nature of involved modes	Modal interaction
All three modes axisymmetric: $k_1 = k_2 = k_3 = 0$	Possible
Only one of them is axymmetric	Impossible
Only one of them is axymmetric: e.g. $k_1 = 0$, $k_2 \neq 0$, $k_3 \neq 0$	Possible if $k_2 = k_3$
All three modes asymmetric: $k_1 \neq 0$, $k_2 \neq 0$, $k_3 \neq 0$	Possible if $\begin{cases} k_1 = k_2 + k_3 \\ k_2 = k_1 + k_3 \\ k_3 = k_1 + k_2 \end{cases}$

k_p is the number of nodal diameters of mode Φ_p, and q_p is the time evolution of mode Φ_p in set (18).

on the numbers of nodal diameters that lead to non-zero resonant terms and thus to a possible energy exchange between the involved modes (fourth line). Then, the particular cases of involved axisymmetric modes and/or asymmetric modes are considered (remaining lines).

These order-two internal resonances are specific to shells with a non-zero curvature, since plates show only order-three internal resonances. Section 5 of this paper is related to the case of Table 3.

4.3.2. Order-three internal resonances

The coupling rules are summarized in Tables 5–7, in a similar manner as for the previous case of order-two internal resonances. Some cubic non-linear terms are always resonant, even if no cubic internal resonance (Eq. (23b)) is fulfilled. An example is a term $q_i q_j^2$, which is resonant in the ith oscillator (of natural frequency ω_i) for any value of the natural frequency ω_j of mode Φ_j, since $\omega_i = \omega_i + \omega_j - \omega_j$. It can be proved (Sridhar et al., 1975; Lacarbonara et al., 2003) that those terms do not lead to large energy exchanges if they are the only ones present in the equations. Thus, only resonant terms specifically related to the cubic internal resonances of Eq. (23b) are considered in Tables 5–7.

These order-three internal resonances are common to any shell; in particular, they are the only internal resonances involved in vibrations of plates (when $\chi = 0$). However, they are of significant importance for shells with small curvature only, since cubic non-linear terms become negligible with respect to quadratic terms for large curvatures ($\varepsilon_c \ll \varepsilon_q$ if R is small compared to a, see Table 1). The case of Table 5 has been recently addressed by Lee et al. (2003) and cases of Tables 6 and 7 extend earlier results of Sridhar et al., 1978), corrected by Yeo and Lee (2002), in the case of circular plates.

Table 5
Rules determining if modal interaction between modes Φ_1 and Φ_2 is possible, when internal resonance $\omega_2 = 3\omega_1$ is fulfilled

$\omega_2 = 3\omega_1$		
Modes	$\Phi_1(\omega_1, k_1)$	$\Phi_2(\omega_2, k_2)$
Resonant terms	$q_1^2 q_2$	q_1^3
Rule	for both res. terms: $\{2k_1, 0\} \cap \{k_1 + k_2, \lvert k_1 - k_2 \rvert\} \neq \emptyset$	

Nature of involved modes	Modal interaction
Both modes axisymmetric: $k_1 = k_2 = 0$	Possible
Only one of them asymmetric	Impossible
Both modes asymmetric: $k_1 \neq 0$, $k_2 \neq 0$	Possible if $\begin{cases} k_2 = k_1 \\ k_2 = 3k_1 \end{cases}$

k_p is the number of nodal diameters of mode Φ_p, and q_p is the time evolution of mode Φ_p in set (18).

Table 6
Rules determining if modal interaction between modes Φ_1, Φ_2 and Φ_3 is possible, when internal resonance $\omega_3 = \omega_1 + 2\omega_2$ is fulfilled

$\omega_3 = \omega_1 + 2\omega_2$		
Modes	$\Phi_1\ (\omega_1,\ k_1)$ $\Phi_2\ (\omega_2,\ k_2)$	$\Phi_3\ (\omega_3,\ k_3)$
Res. terms	$q_2^2 q_3$	$q_1 q_2^2$
Rule	for all three res. terms: $\begin{cases} \{k_1 + k_2, \mid k_1 - k_2 \mid\} \cap \{k_2 + k_3, \mid k_2 - k_3 \mid\} \neq \emptyset \\ \{2k_2, 0\} \cap \{k_1 + k_3, \mid k_1 - k_3 \mid\} \neq \emptyset \end{cases}$	

Nature of involved modes	Modal interaction
All three modes axisymmetric: $k_1 = k_2 = k_3 = 0$	Possible
Only mode Φ_1 asymmetric: $k_1 \neq 0$, $k_2 = k_3 = 0$	Impossible
Only mode Φ_2 asymmetric: $k_2 \neq 0$, $k_1 = k_3 = 0$	Possible $\forall k_2$
Only mode Φ_3 asymmetric: $k_3 \neq 0$, $k_1 = k_2 = 0$	Impossible
Only mode Φ_1 axisymmetric: $k_1 = 0$, $k_2 \neq 0$, $k_3 \neq 0$	Possible if $k_3 = 2k_2$
Only mode Φ_2 axisymmetric: $k_2 = 0$, $k_1 \neq 0$, $k_3 \neq 0$	Possible if $k_1 = k_3$
Only mode Φ_3 axisymmetric: $k_3 = 0$, $k_1 \neq 0$, $k_2 \neq 0$	Possible if $k_1 = 2k_2$
All three modes asymmetric: $k_1 \neq 0$, $k_2 \neq 0$, $k_3 \neq 0$	Possible if $\begin{cases} k_1 = k_3\ \forall k_2 \\ k_1 + k_3 = 2k_2 \\ k_1 = 2k_2 + k_3 \\ k_3 = k_2 + k_1 \end{cases}$

k_p is the number of nodal diameters of mode Φ_p, and q_p is the time evolution of mode Φ_p in set (18).

Table 7
Rules determining if modal interaction between modes Φ_1, Φ_2, Φ_3 and Φ_4 is possible, when internal resonance $\omega_4 = \omega_1 + \omega_2 + \omega_3$ is fulfilled

$\omega_4 = \omega_1 + \omega_2 + \omega_3$				
Modes	$\Phi_1(\omega_1, k_1)$	$\Phi_2(\omega_2, k_2)$	$\Phi_3(\omega_3, k_3)$	$\Phi_4(\omega_4, k_4)$
Res. terms	$q_2 q_3 q_4$	$q_1 q_3 q_4$	$q_1 q_2 q_4$	$q_1 q_2 q_3$
Rule	for all four res. terms: $\{k_1 + k_2, \mid k_1 - k_2 \mid\} \cap \{k_3 + k_4, \mid k_3 - k_4 \mid\} \neq \emptyset$			

Nature of involved modes	Modal interaction
All three modes axisymmetric: $k_1 = k_2 = k_3 = 0$	Possible
Only one of them asymmetric	Impossible
Only two asym.: e.g. $k_1 \neq 0$, $k_2 \neq 0$, $k_3 = k_4 = 0$	Possible if $k_1 = k_2$
Only one axisym.: $k_p = 0$, $k_q \neq 0$ $(q \neq p)$	Possible if $\begin{cases} k_1 = k_2 + k_3 \\ k_2 = k_1 + k_3 \\ k_3 = k_1 + k_2 \end{cases}$
All asym.: $k_1 \neq 0$, $k_2 \neq 0$, $k_3 \neq 0$, $k_4 \neq 0$	Possible if $\begin{cases} k_1 + k_2 = k_3 + k_4 \\ k_1 + k_3 = k_2 + k_4 \\ k_1 + k_4 = k_2 + k_3 \\ k_1 = k_2 + k_3 + k_4 \\ k_2 = k_1 + k_3 + k_4 \\ k_3 = k_1 + k_2 + k_4 \\ k_4 = k_1 + k_2 + k_3 \end{cases}$

k_p is the number of nodal diameters of mode Φ_p, and q_p is the time evolution of mode Φ_p in set (18).

4.4. Influence of curvature

Some numerical values of coefficients are now exhibited to evaluate the dependence of coefficients β^s_{pq} and Γ^s_{pqu} on the curvature of the shell. They were computed numerically using Eqs. (20) and (21) with the analytical expressions of the mode shapes of Appendix A and B.

Table 8
Numerical values of coefficients of quadratic resonant terms in the case of the 1:1:2 internal resonance between two companion asymmetric mode $(k,0)$ and the first axisymmetric mode $(0,1)$, as functions of curvature parameter χ and for $\nu = 0.33$

Mode (k,n)	Coef. of res. terms	Curvature parameter χ			
		10^{-9}	100	1000	10000
$(2,0)$	$\alpha_1 = \alpha_2$	1.9555	1.9562	1.9555	1.9453
	$\alpha_3 = \alpha_4$	0.9778	0.9782	0.9778	0.9727
$(3,0)$	$\alpha_1 = \alpha_2$	5.7070	5.7086	5.7122	5.6783
	$\alpha_3 = \alpha_4$	2.8535	2.8543	2.8562	2.8393
$(4,0)$	$\alpha_1 = \alpha_2$	11.201	11.203	11.212	11.166
	$\alpha_3 = \alpha_4$	5.6006	5.6016	5.6059	5.5833
$(5,0)$	$\alpha_1 = \alpha_2$	18.414	18.416	18.427	18.389
	$\alpha_3 = \alpha_4$	9.2072	9.2081	9.2137	9.1952
$(6,0)$	$\alpha_1 = \alpha_2$	27.333	27.335	27.346	27.328
	$\alpha_3 = \alpha_4$	13.667	13.668	13.674	13.665
$(7,0)$	$\alpha_1 = \alpha_2$	37.952	37.953	37.964	37.967
	$\alpha_3 = \alpha_4$	18.977	18.977	18.983	18.985

The $\{\alpha_i\}_{i=1\ldots4}$ are defined by Eqs. (25a)–(25c); $\alpha_1 = -\beta^1_{13} - \beta^1_{31} = \alpha_2 = -\beta^1_{23} - \beta^1_{32}$ and $\alpha_3 = -\beta^3_{11} = \alpha_4 = -\beta^3_{22}$. Twelve modes Υ_b have been retained in Eq. (20), in order to obtain a 5-digit precision.

Table 8 shows several values of quadratic coefficients α_i of resonant terms in the case of the 1:1:2 internal resonance treated in Section 5 (The coefficients are defined by Eqs. (25a)–(25c)). Fig. 9 presents the evolution of the relative value of coefficients α_i, that is the ratio of α_i to its value for $\chi = 10^{-9}$. One can observe that these quadratic coefficients depend only slightly on the curvature parameter χ. Moreover, the relative evolution with respect to χ of coefficient $\alpha_1 = \alpha_2$ is identical to that of $\alpha_3 = \alpha_4$, for a given value of the number k of nodal diameters of the companion modes. This is a consequence of the fact that for a given value of k, the $\{\alpha_i\}_{i=1,\ldots,4}$ all depend on the same modal shapes (Φ_{k0} and Φ_{01}).

Table 9 shows the only cubic coefficient that is involved in a single axisymmetric mode vibration. It does not depends on χ. The same table and Fig. 10 shows coefficient of the 1:1 internal resonance between two companion purely asymmetric modes with k nodal diameters (and no nodal circles). They depend very

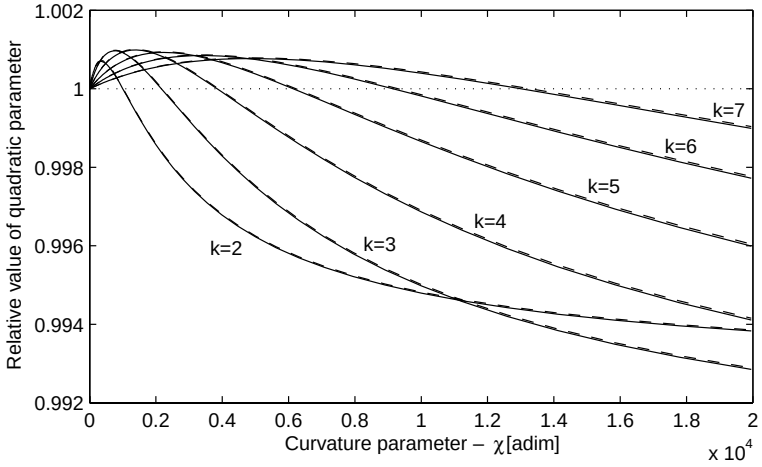


Fig. 9. Evolution of coefficients of quadratic resonant terms of Table 8 with respect to curvature parameter χ, for $k \in \{2,\ldots 7\}$: (—) ratio of $\alpha_1 = \alpha_2$ to their value for $\chi = 10^{-9}$ and (–) ratio of $\alpha_3 = \alpha_4$ to their value for $\chi = 10^{-9}$.

Table 9
Numerical values of coefficients of cubic resonant term in the case of a single axisymmetric mode $(0,n)$ or in the case of the 1:1 internal resonance between two companion asymmetric mode $(k,0)$, with respect to curvature parameter χ and for $\nu = 0.33$

Mode (k,n)	10^{-9}	Curvature parameter χ		
		100	1000	10,000
(0,1)		8.5287		
(0,2)		163.77		
(0,3)		1076.6		
(2,0)	1.8966	1.8985	1.9053	1.9093
(3,0)	16.984	17.304	17.987	18.121
(4,0)	70.001	70.203	71.724	77.034
(5,0)	202.83	203.32	207.26	226.33
(6,0)	476.77	477.68	485.36	531.57
(7,0)	975.31	976.78	989.45	1078.1

Twelve modes Υ_b have been retained in Eq. (21), in order to obtain a five-digit precision.

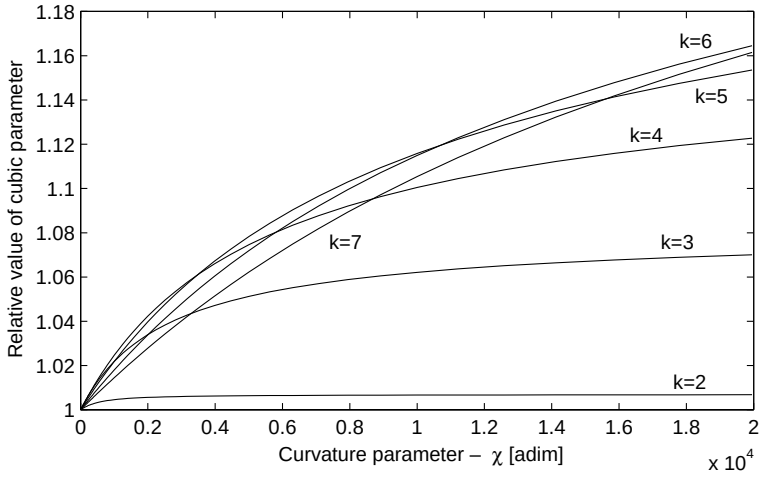


Fig. 10. Evolution of coefficients of cubic resonant terms of Table 9, related to purely asymmetric modes with k nodal diameters, with respect to curvature parameter χ. The ratio between the coefficient to its value for $\chi = 10^{-9}$ is plotted, for $k \in \{2,\dots 7\}$.

slightly on the curvature parameter χ. The numerical values of this latter case are in agreement with those computed in Touzé et al. (2002) for a circular plate.

One can conclude that coefficients are almost constant as a function of χ. It is a consequence of the fact that the shell mode shapes slightly depend on curvature, as shown in Section 3.1. Thus, the dependence of the dynamics of the shell upon its geometry is mainly governed by the value of ε_q (Eq. (8b)), since ε_c is a constant with respect to the curvature (Eq. (8c)).

5. Application: the case of a one-to-one-to-two internal resonance

This section is devoted to the analysis of a system exhibiting a one-to-one-to-two (1:1:2) internal resonance, corresponding to the interaction between two companion asymmetric mode with an axisymmetric mode, whose natural frequency is nearly equal to twice that of the asymmetric ones. This specific internal

resonance is studied here because it has been observed on a real shell at the laboratory, with energy transfer between the first $(0,1)$ axisymmetric mode and the sixth $(6,0)$ asymmetric. Fig. 11 shows the vibration pattern measured with a scanning laser vibrometer, when the structure is excited at its center by means of a sinusoidal forcing. The vibrations patterns resulting from two excitation conditions—related to two frequencies of excitations close to the natural frequency of the $(0,1)$ mode—are shown on Fig. 11, with and without coupling with one of the companion asymmetric $(6,0)$ modes. Precise measurements and model fitting will be reported in a forthcoming paper.

Two-to-one internal resonance occurs in many different physical systems and has been already studied by a number of investigators (see e.g. Nayfeh and Balachandran, 1989; Nayfeh, 2000, and references therein, for a quick survey including references on spring pendulum, ships, surface waves in closed basins, etc.). For mechanical systems displaying geometrical non-linearities, this specific resonance has been studied both theoretically and experimentally for a structure composed of two slender beams and two dense masses, which were adjusted so that the first two natural frequencies were in the ratio 1:2 (Haddow et al., 1984; Nayfeh and Zavodney, 1988). The two-dof dynamical system has also been studied by Miles (1984), Yamamoto and Yasuda (1977), and the particular phenomenon of saturation was exhibited. As structures with curvature display quadratic non-linearity, 1:2 resonance has naturally been studied for the vibrations of arches and suspended cables (see e.g. Tien et al., 1994; Benedettini et al., 1995).

In the field of circular cylindrical shell vibrations, Nayfeh and Raouf (1987) performed a similar study, as they investigated the interaction between an axisymmetric mode and the two configurations of an asymmetric mode. However, they only considered the perfect case of an infinitely long cylinder. In particular they did not take into account the small detuning that necessary occur between the two preferential configurations in a real system. We will show that these imperfections have a fundamental role for explaining the experimentally observed coupling. More recently, they proposed a second-order solution (Chin and Nayfeh, 2001). Robie et al. (1999) also studied the 1:2 internal resonance, but they limited their study to free undamped vibrations, and considered one asymmetric configuration only. Alhazza (2002) analyzed the 1:2 resonance for a doubly-curved cross-ply shallow shell. Finally, a 1:1:1:2 resonance in circular cylindrical shells has been studied by Amabili et al., but the forcing was considered on one preferential configuration, thus naturally leading to coupled solutions with the first and third axisymmetric mode for any vibration amplitude (Amabili et al., 2000, Pellicano et al., 2000). Moreover, the two configurations were supposed to have exactly equal eigenfrequencies.

The present developments are aimed at filling the gap between the previous studies and sheding light on the relevance of the parameters that are specifically connected to the imperfection of the shell. More specifically, it will be shown that those parameters are crucial for understanding the nature of the coupled

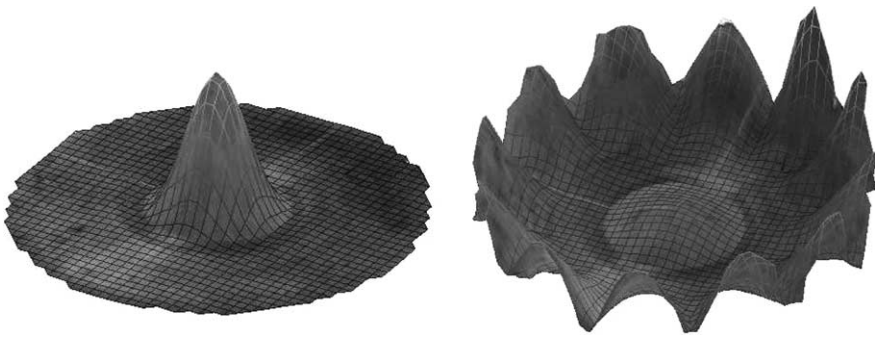


Fig. 11. Vibration pattern with (right) and without (left) coupling between the $(0,1)$ mode and a purely asymmetric $(6,0)$ mode, measured on a real shell with a scanning laser vibrometer. The geometry of the shell is defined by $a = 300\,\text{mm}$, $R = 1.515\,\text{m}$ and $h = 1\,\text{mm}$.

regime. It will be demonstrated that the energy transfer is specific to one of the companion asymmetric modes and that no traveling wave appear as long as the cubic terms are effectively negligible.

The spherical shell is assumed to be excited by an external sinusoidal force located at its center, whose frequency Ω is chosen close to the natural frequency (denoted here by ω_3) of an axisymmetric mode $(0,n')$ of n' nodal circles. The curvature parameter χ is chosen so that an internal resonance exist between mode $(0,n')$ and two companion asymmetric modes (k,n) of frequencies ω_1 and ω_2, so that $\omega_3 \simeq 2\omega_1 \simeq 2\omega_2$. Fig. 3 shows that these internal resonances occur for many values of χ. For example, mode $(0,1)$ can be involved in a 1:1:2 internal resonance between any of the asymmetric modes $(k,0)$ with no nodal circles. In the following, a reduced order model is deduced from the set (18) and we focus on a first-order perturbative solution. As a consequence, (i) only the modes involved in internal resonance are retained, (ii) the cubic terms are neglected with respect to the others, according to the values of the parameters ε_q and ε_c (see Table 1) and (iii) all non-resonant terms are dropped. The transverse displacement $w(r,\theta,t)$ is then written

$$w(r,\theta,t) = R_{kn}(r)(q_1(t)\cos k\theta + q_2(t)\sin k\theta) + R_{0n'}q_3(t), \tag{24}$$

where q_1 and q_2 are related to the asymmetric modes and q_3 to the axisymmetric. $R_{kn}(r)$ and $R_{0n'}(r)$ are defined in Appendix A. The $\{q_i\}_{i=1,\ldots,3}$ are solutions of the following set, deduced from (18):

$$\ddot{q_1} + \omega_1^2 q_1 = \varepsilon_q[\alpha_1 q_1 q_3 - 2\mu_1 \dot{q_1}], \tag{25a}$$

$$\ddot{q_2} + \omega_2^2 q_2 = \varepsilon_q[\alpha_2 q_2 q_3 - 2\mu_2 \dot{q_2}], \tag{25b}$$

$$\ddot{q_3} + \omega_3^2 q_3 = \varepsilon_q[\alpha_3 q_1^2 + \alpha_4 q_2^2 - 2\mu_3 \dot{q}_3 + Q\cos\Omega t]. \tag{25c}$$

The forcing terms of the first two oscillators (25a) and (25b) vanish since the corresponding modes have a node at the center of the shell. The term proportional to q_3^2 in Eq. (25c) is not considered since it is non-resonant. The reduced-order model defined above is justified because the present study is focused on the loss of stability of the single degree-of-freedom (sdof) solution (defined by the directly excited axisymmetric mode only, $q_1(t) \equiv q_2(t) \equiv 0$). A first-order perturbative development is then sufficient and the formalism of non-linear normal modes need not to be used (Nayfeh and Nayfeh, 1994). This would not be the case if one was interested in predicting the hardening or softening behavior of a single mode. In this situation, it would be necessary to retain a number of additional oscillators in the model, the cubic terms as well as the non-resonant terms, as shown for example in the case of circular cylindrical shells by Amabili et al. (1999) or in a general case by Touzé et al. (2004) with the formalism of non-linear modes.

Coefficients $\{\alpha_i\}_{i=1,\ldots,4}$ can be computed from the β_{qs}^p expressed in Eq. (20). In a perfect case, one obtains $\alpha_1 = \alpha_2$, and $\alpha_3 = \alpha_4$, as shown in Table 8. However, for the sake of generality, the $\{\alpha_i\}_{i=1,\ldots,4}$ are kept variable in the following. To express the internal resonance relationships, we introduce two internal detuning parameters σ_0 and σ_1

$$\omega_2 = \omega_1 + \varepsilon_q\sigma_0, \tag{26a}$$

$$\omega_3 = 2\omega_1 + \varepsilon_q\sigma_1. \tag{26b}$$

One can notice that: $\omega_3 = 2\omega_2 + \varepsilon_q(\sigma_1 - 2\sigma_0)$. Finally an external detuning parameter σ_2 is introduced to express the nearness of the forcing frequency with the axisymmetric natural frequency

$$\Omega = \omega_3 + \varepsilon_q\sigma_2. \tag{27}$$

5.1. Multiple scale solution

System (25) is solved by the method of multiple scales. To the first-order, and for $j = 1,2,3$

$$q_j(t) = q_{j1}(T_0,T_1) + \varepsilon_q q_{j2}(T_0,T_1) + O(\varepsilon_q^2), \tag{28}$$

where $T_0 = t$ and $T_1 = \varepsilon_q t$. The first-order equations lead to express the $\{q_{j1}\}_{j=1,2,3}$ as

$$q_{j1}(T_0, T_1) = \frac{1}{2} a_j(T_1) \exp(\mathrm{i}\theta_j(T_1)) \exp(\mathrm{i}\omega_j T_0) + \text{c.c.}, \tag{29}$$

where c.c. stands for complex conjugate. Polar form is used to express the amplitude of the first-order solutions, which depends on the slow time scale T_1. Introducing (29) into the second-order equations leads to the so-called solvability condition, which can be written as a six-dimensional dynamical system by separating real and imaginary parts. Finally, the following variables allows definition of an autonomous dynamical system:

$$\gamma_1 = \sigma_1 T_1 + \theta_3 - 2\theta_1, \quad \gamma_2 = (\sigma_1 - 2\sigma_0) T_1 + \theta_3 - 2\theta_2, \quad \gamma_3 = \sigma_2 T_1 - \theta_3. \tag{30}$$

It reads

$$a_1' = -\mu_1 a_1 + \frac{\alpha_1 a_1 a_3}{4\omega_1} \sin\gamma_1, \tag{31a}$$

$$\gamma_1' = \sigma_1 - \frac{\alpha_3 a_1^2}{4\omega_3 a_3} \cos\gamma_1 - \frac{\alpha_4 a_2^2}{4\omega_3 a_3} \cos\gamma_2 - \frac{Q}{2\omega_3 a_3} \cos\gamma_3 + \frac{\alpha_1 a_3}{2\omega_1} \cos\gamma_1, \tag{31b}$$

$$a_2' = -\mu_2 a_2 + \frac{\alpha_2 a_2 a_3}{4\omega_2} \sin\gamma_2, \tag{31c}$$

$$\gamma_2' = \sigma_1 - 2\sigma_0 - \frac{\alpha_3 a_1^2}{4\omega_3 a_3} \cos\gamma_1 - \frac{\alpha_4 a_2^2}{4\omega_3 a_3} \cos\gamma_2 - \frac{Q}{2\omega_3 a_3} \cos\gamma_3 + \frac{\alpha_2 a_3}{2\omega_2} \cos\gamma_2, \tag{31d}$$

$$a_3' = -\mu_3 a_3 - \frac{\alpha_3 a_1^2}{4\omega_3} \sin\gamma_1 - \frac{\alpha_4 a_2^2}{4\omega_3} \sin\gamma_2 + \frac{Q}{2\omega_3} \sin\gamma_3, \tag{31e}$$

$$\gamma_3' = \sigma_2 + \frac{\alpha_3 a_1^2}{4\omega_3 a_3} \cos\gamma_1 + \frac{\alpha_4 a_2^2}{4\omega_3 a_3} \cos\gamma_2 + \frac{Q}{2\omega_3 a_3} \cos\gamma_3, \tag{31f}$$

where $(\cdot)'$ stands for the derivation with respect to T_1.

5.2. Fixed points

Fixed points for Eq. (31) are obtained by cancelling the left-hand side terms, which involve a derivative with respect to time. There are a priori four kinds of fixed points:

(i) *sdof solution.* It corresponds to the case where $a_1 = a_2 = 0$: no energy transfer between modes occur and the response of the system is governed by the directly excited axisymmetric mode only. Its amplitude is given by

$$a_3 = \frac{Q}{2\omega_3 \sqrt{\sigma_2^2 + \mu_3^2}}, \tag{32}$$

(ii) *C1 solution*. It corresponds to a coupling between the axisymmetric mode and the first asymmetric configuration, thus $a_1 \neq 0$, and $a_2 = 0$.

(iii) *C2 solution.* The coupling is here with the second asymmetric configuration: $a_1 = 0$, and $a_2 \neq 0$.

(iv) *C3 solution*. Coupling with both asymmetric configurations at the same time, leading to $a_1 \neq 0$ and $a_2 \neq 0$. It will be shown next that this solution exists only in the perfect case.

Analytical expressions for the *C1* and *C2* solutions are easily available with a little algebra, which is not reproduced here (see e.g. Nayfeh and Raouf, 1987; Nayfeh and Mook, 1979; Haddow et al., 1984). One then obtains:

- *C1 solution:*

$$a_3 = \frac{2\omega_1}{\alpha_1}\sqrt{4\mu_1^2 + (\sigma_1 + \sigma_2)^2}, \tag{33a}$$

$$a_1 = 2\sqrt{-\Gamma_1 \pm \sqrt{\frac{Q^2}{4\alpha_3^2} - \Gamma_2^2}}, \tag{33b}$$

$$\text{with :} \quad \Gamma_1 = \frac{2\omega_1\omega_3}{\alpha_1\alpha_3}(2\mu_1\mu_3 - \sigma_2(\sigma_1 + \sigma_2)), \tag{33c}$$

$$\text{and :} \quad \Gamma_2 = \frac{2\omega_1\omega_3}{\alpha_1\alpha_3}(2\sigma_2\mu_1 + \mu_3(\sigma_1 + \sigma_2)). \tag{33d}$$

- *C2 solution:*

$$a_3 = \frac{2\omega_2}{\alpha_2}\sqrt{4\mu_2^2 + (\sigma_1 - 2\sigma_0 + \sigma_2)^2}, \tag{34a}$$

$$a_2 = 2\sqrt{-\Gamma_3 \pm \sqrt{\frac{Q^2}{4\alpha_4^2} - \Gamma_4^2}}, \tag{34b}$$

$$\text{with :} \quad \Gamma_3 = \frac{2\omega_2\omega_3}{\alpha_2\alpha_4}(2\mu_2\mu_3 - \sigma_2(\sigma_1 - 2\sigma_0 + \sigma_2)), \tag{34c}$$

$$\text{and :} \quad \Gamma_4 = \frac{2\omega_2\omega_3}{\alpha_2\alpha_4}(2\sigma_2\mu_2 + \mu_3(\sigma_1 - 2\sigma_0 + \sigma_2)). \tag{34d}$$

One can notice that the symmetry of the original equations (25) allows derivation of the expression for the *C2* solution from the expression found for *C1*. The symmetry of the system is of great help for the understanding and analysis of energy transfer, as shown next.

The *C3* case is considered by keeping all amplitudes different from zero. However, the operations that lead to Eqs. (33a) and (34a) are still possible. Thus, in the more general case, when the two asymmetric configurations are eventually present in the vibration, a_3 can take the two different values given by (33a) and (34a). Moreover it can be shown that if a_3 is equal to (33a) (respectively, equal to (34a)), then γ_2 (respectively, γ_1) is undefined and $a_2 = 0$ (respectively, $a_1 = 0$) is the only possible case. As a consequence, no other solutions than the ones already described (sdof, *C1* and *C2*) are available, except when Eqs. (33a) and (34a) are simultaneously fulfilled, which is true only in the perfect case (defined by: $\mu_1 = \mu_2$, $\alpha_1 = \alpha_2$, and $\omega_1 = \omega_2$, which implies $\sigma_0 = 0$). The stability analysis confirms these conclusions, as well as numerical simulations which were conducted with the software DsTool (Guckenheimer et al., 1995).

5.3. Stability analysis

A linear stability analysis is performed by computing the Jacobian matrix $\mathscr{J}$ of Eq. (31). We first investigate the stability of the sdof solution. The eigenvalues are

$$\lambda_{1,2}^{\mathrm{sdof}} = -\mu_3 \pm \mathrm{i}\sigma_2, \tag{35a}$$

$$\lambda_1^{\mathrm{C1}} = -\mu_1 + \frac{\alpha_1 a_3}{4\omega_1}\sin\gamma_1, \tag{35b}$$

$$\lambda_2^{\mathrm{C1}} = -\frac{\alpha_1 a_3}{2\omega_1}\sin\gamma_1, \tag{35c}$$

$$\lambda_1^{\mathrm{C2}} = -\mu_2 + \frac{\alpha_2 a_3}{4\omega_2}\sin\gamma_2, \tag{35d}$$

$$\lambda_2^{\mathrm{C2}} = -\frac{\alpha_2 a_3}{2\omega_2}\sin\gamma_2. \tag{35e}$$

The superscripts indicate that each pair of eigenvalues can be easily related to: (i) the stability of the sdof solution with respect to perturbations contained within the subspace $a_1 = a_2 = 0$ (sdof case), (ii) its stability with respect to perturbations caused by the presence of the first asymmetric configuration (C1 case), (iii) its stability with respect to perturbations caused by the second asymmetric configuration (C2 case). The simple form of Eq. (35a–e) is a direct consequence of the relative decoupling and symmetry of the initial equations (25). By forming the products $\lambda_1^{\mathrm{C1}}.\lambda_2^{\mathrm{C1}}$ and $\lambda_1^{\mathrm{C2}}.\lambda_2^{\mathrm{C2}}$, and eliminating γ_1 and γ_2 in favor of the other parameters, one can exhibit two stability conditions for the sdof solutions:

$$a_3 \leqslant L_1(\sigma_2), \quad \text{where } L_1(\sigma_2) = \frac{2\omega_1}{\alpha_1}\sqrt{4\mu_1^2 + (\sigma_1 + \sigma_2)^2}, \tag{36}$$

$$a_3 \leqslant L_2(\sigma_2), \quad \text{where } L_2(\sigma_2) = \frac{2\omega_2}{\alpha_2}\sqrt{4\mu_2^2 + (\sigma_1 - 2\sigma_0 + \sigma_2)^2}, \tag{37}$$

with a_3 defined by Eq. (32). These stability conditions have been reported in Fig. 12, where the sdof solutions is unstable in the gray shaded regions.

In the perfect case—i.e., defined by the complete identity of the two configurations (i.e. $\alpha_1 = \alpha_2$, $\omega_1 = \omega_2$ and $\mu_1 = \mu_2$), the two curves $L_1(\sigma_2)$ and $L_2(\sigma_2)$ are merged. Hence both configurations are simultaneously excited when the sdof curve crosses $L_1 \equiv L_2$. It can then be shown that their amplitudes verify the following relationship:

$$a_1^2 + a_2^2 = -4\Gamma_1 + \sqrt{16\Gamma_1^2 - \left[\frac{64\omega_1^2\omega_3^2}{\alpha_1^2\alpha_3^2}(4\mu_1^2 + (\sigma_1 + \sigma_2)^2)(\mu_3^2 + \sigma_2^2) - \frac{4Q^2}{\alpha_3^2}\right]} \tag{38}$$

An infinity of coupled solutions are available: any solution that verify Eq. (38). This has been verified numerically. The reader interested in the perfect case is referred to Nayfeh and Raouf (1987) for a complete study.

In real situations, it is impossible to ensure perfectness, and slight perturbations are always present that break the precedent results and keep the curves $L_1(\sigma_2)$ and $L_2(\sigma_2)$ distinct, so that the situation depicted in Fig. 12 is generic. The discussion is restricted to positive values of σ_0, because the ordering of the configurations is made by their natural frequencies.

The stability of the C1 and C2 solutions is now addressed. In Fig. 12, if the sdof solution is followed from $\sigma_2 < 0$ for increasing values, it first crosses L_1 at $\sigma_2 = -1.5$, so that a C1 solution is obtained, whose

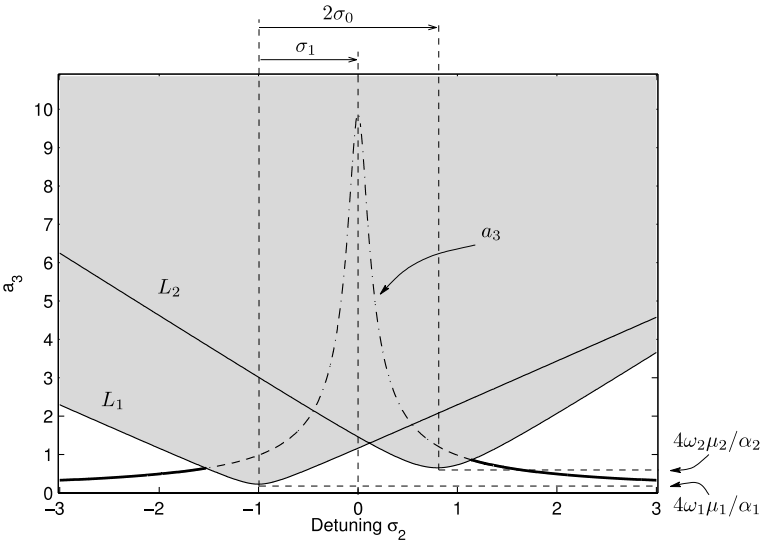


Fig. 12. Stability of the sdof solution with respect to the perturbations caused by the first configuration (L_1 curve), and by the second configuration (L_2 curve). The figure is made with $\alpha_1 = 7$, $\alpha_2 = 5$, $\mu_1 = \mu_3 = 0.1$, $\mu_2 = 0.2$, $Q = 16$, $\omega_1 = 4$, $\omega_2 = 4.09$, $\omega_3 = 8.1$.

stability is studied by substituting for Eqs. (33a) and (33b) in the Jacobian matrix $\mathscr{J}$. The eigenvalues are found to be solutions of

$$P(\lambda) = \det(\mathscr{J} - \lambda I) = \left(-\mu_2 + \frac{\alpha_2 a_3}{4\omega_2}\sin\gamma_2 - \lambda\right)\left(-\frac{\alpha_2 a_3}{2\omega_2}\sin\gamma_2 - \lambda\right)P_{C2}(\lambda), \tag{39}$$

where $P_{C2}(\lambda)$ governs the eigenvalues of the C1 solution with respect to perturbations contained within the subspace $a_2 = 0$. Hence the perturbations created by the presence of the second configuration are completely described by the first two eigenvalues, which are exactly equal to that obtained when studying the sdof solution (see Eqs. (35d) and (35e)). The C1 solution is thus stable as long as $a_3 \leqslant L_2(\sigma_2)$ with a_3 given now by Eq. (33a). For the C1 solution, a_3 (given by Eq. (33a)) takes exactly the value given by the stability condition L_1 (Eq. (36)), so that it can be read in Fig. 12 that the C1 solution is stable as long as $L1$ does not cross $L2$. In Fig. 12, the crossing occurs at $\sigma_2 = 0.30$, where a stability exchange is observed: the C1 solution loses its stability in favor of the C2 solution. Thanks to the symmetry of the system, the discussion is equivalent when following the sdof solution for decreasing values from $\sigma_2 > 0$, by replacing C1 by C2.

It has been demonstrated that the discussion on the stability can be made by simply following the values taken by the amplitude a_3 of the directly excited axisymmetric mode, and that the coupling occurs either with the first configuration, or with the second. The imperfections of the system avoid simultaneous energy transfer to the two configurations. A stability exchange occurs. Hence travelling waves are not possible.

5.4. Generalized stability curves

Fig. 13 displays the different solutions for a typical case. All branches of solutions are obtained analytically from the results of Sections 5.2 and 5.3 and have been systematically verified by numerical simulations using the software DsTool. When increasing σ_2, one observes first the sdof solution. At $\sigma_2 = -1.5$, the first coupling occurs, with the first asymmetric configuration: a_1 follows the C1 branch, as well as a_3. At $\sigma_2 = \hat{\sigma}_2 = 0.12$, the stability exchange occurs: a_1 goes down to zero while a_2 grows up to the C2 branch,

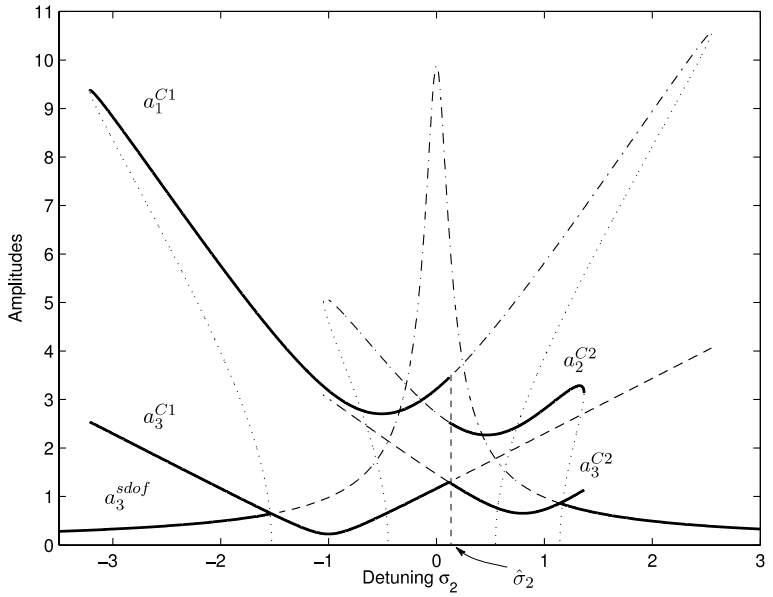


Fig. 13. Generalized stability curve for the case: $\alpha_1 = 7$, $\alpha_2 = 5$, $\alpha_3 = 3$, $\alpha_4 = 4$, $\mu_1 = \mu_3 = 0.1$, $\mu_2 = 0.2$, $Q = 16$, $\omega_1 = 4$, $\omega_2 = 4.09$, $\omega_3 = 8.1$. Stable branches are plotted with solid lines, all other branches are unstable.

and a_3 follows the C2 branch until $\sigma_2 = 1.36$. Hysteretic behaviour is present: when decreasing the excitation frequency, the second configuration is excited first for $\sigma_2 = 1.14$, the stability exchange occurs at the same value $\sigma_2 = 0.12$, from which the first configuration is excited until $\sigma_2 = -3.2$.

A complete parametric study of all possible cases is difficult to formulate because of the size of the parameter space. Nonetheless, we will give now briefly a few guidelines of the possible features by changing two important physical parameters: the internal detuning between the two configurations σ_0 and the amplitude of the forcing Q.

The stability analysis have proven that a mere glance at the relative position of the two stability curves L_1 and L_2 is sufficient to have a comprehensive idea of which coupling will occur. In particular, if e.g. configuration 1 is much more damped than the other, or if the coupling coefficient α_1 is small (see Fig. 12), the stability curve L_1 is reached for large Q values only, and thus the main observation is related to a coupling with the second configuration.

Fig. 14 shows the different behaviour exhibited when increasing the internal detuning σ_0, when all other coefficients are related to a perfect case (i.e. $\alpha_1 = \alpha_2$, $\alpha_3 = \alpha_4$, $\mu_1 = \mu_2 = \mu_3$). It is assumed in addition that $\sigma_1 = 1$.

When σ_0 is small (Fig. 14(a)–(b): $\sigma_0 = 0.1$). The second configuration is mainly observed because the L_2 curve is under L_1 in a wide instability range: $\hat{\sigma}_2 \leqslant \sigma_2 \leqslant 0.26$, where $\hat{\sigma}_2 = L_1 \cap L_2 = -1.17$ represents the intersection point. An opposite result would have been observed by setting $\sigma_1 = -1$. Increasing σ_0 leads to move the intersection point $\hat{\sigma}_2$. At $\sigma_0 = 1.1$ (Fig. 14(c)–(d)), the C2 branch becomes very short, and the coupling mainly occurs with the first configuration. As L_2 still crosses the sdof solution around $\sigma_2 = 1.1$, a short C2 branch is observed. In this specific case, an increasing sweep of the excitation frequency will then produce successively: the sdof solution ($\sigma_2 \leqslant -1.17$), the C1 solution ($-1.17 \leqslant \sigma_2 \leqslant 0.11$), the C2 solution ($0.11 \leqslant \sigma_2 \leqslant 0.31$), the sdof solution ($0.31 \leqslant \sigma_2 \leqslant 0.96$), the C2 solution ($0.96 \leqslant \sigma_2 \leqslant 1.40$) and finally the sdof solution. For higher values of σ_0 (Fig. 14(e)–(f): $\sigma_0 = 1.4$), no stable branches corresponding to C2 are present. Hence the coupling with the second configuration will not occur anymore. However, the effect of the second configuration is still present, unless the limiting value of the C1 branch defined by

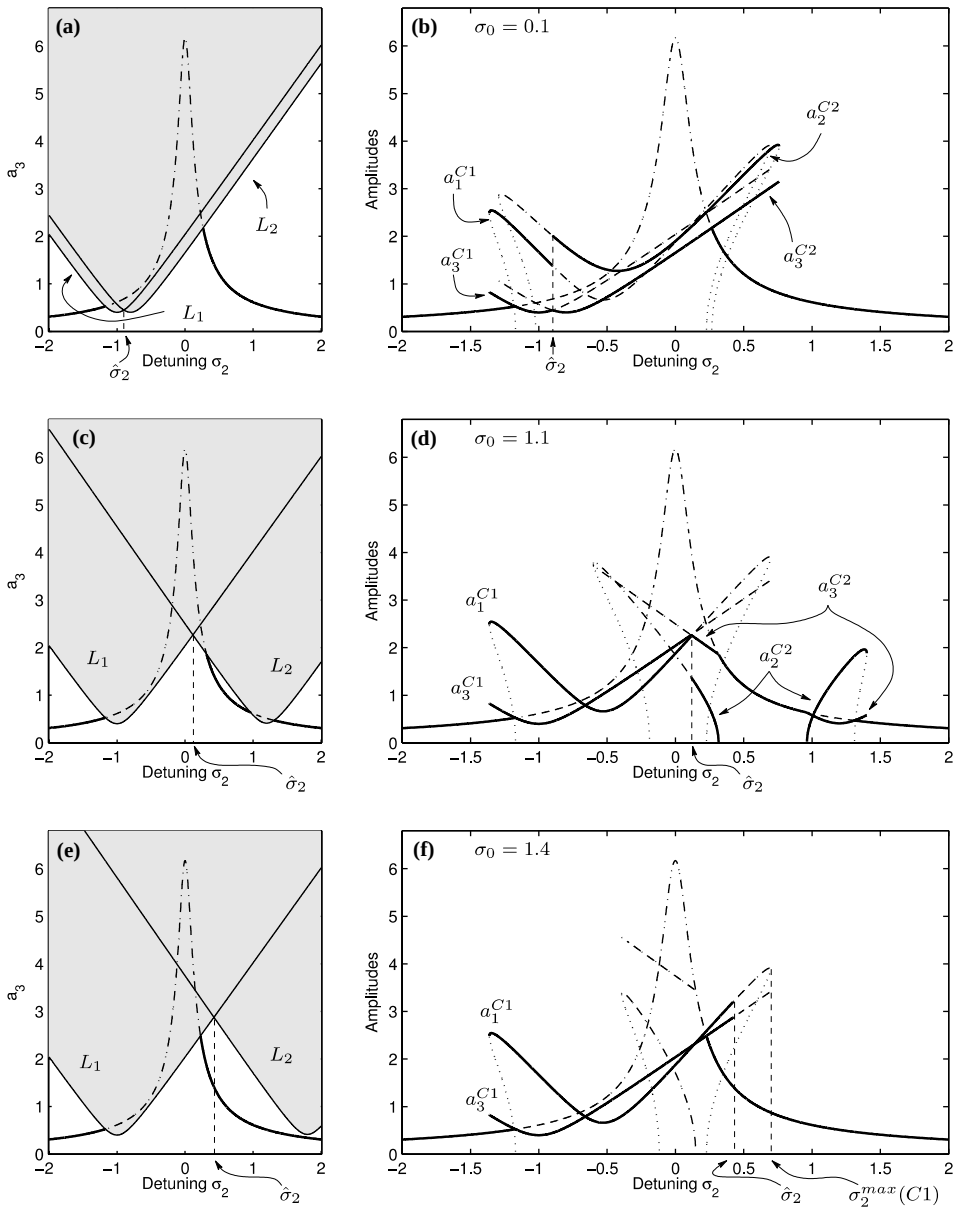


Fig. 14. Relative positions of the L_1 and L_2 stability curves (left column), and variation of the branches of solutions (right column), for increasing values of the internal detuning parameter σ_0. Other values are fixed at: $\alpha_1 = \alpha_2 = 4$, $\alpha_3 = \alpha_4 = 5$, $\mu_i = 0.1$, $Q = 10$, $\omega_1 = 4$, $\sigma_1 = 1$.

$$\sigma_2^{\max}(\mathrm{C1}) = \left(\frac{Q\alpha_1}{4\omega_1\omega_3} - \mu_3\sigma_1\right) \Big/ (2\mu_3 + \mu_1) \tag{40}$$

is lower than $\hat{\sigma}_2$. One can see in Fig. 14(f) that the stable portion of the C1 branch is shortened because of the second configuration. If one increases σ_0 further, the situation where $\hat{\sigma}_2 > \sigma_2^{\max}(\mathrm{C1})$ happens, the stable

portion of the C1 branch is not shortened and all happens as if only the first configuration was present in the dynamics.

The variations of the amplitudes of the solutions can be represented as functions of Q in order to highlight the phenomenon of saturation of the directly excited mode. Eq. (33a,b) and (34a,b) are then plotted for a given σ_2 and a variable Q. The value $\hat{\sigma}_2 = L_1 \cap L_2$ which determines the stability exchange, is independent of Q. Thus for a given external detuning, no stability exchange occurs, so that representation of this curves are the same as the already studied 1:2 resonance (see e.g. Nayfeh and Raouf, 1987; Nayfeh and Mook, 1979; Haddow et al., 1984).

5.5. Solution for the deflection

In steady state, the deflection of the shell is governed by Eq. (24), with the time functions for the three modes defined at first-order by

$$q_1(t) = a_1 \cos\left(\frac{\Omega}{2}t - \frac{\gamma_1 + \gamma_3}{2}\right), \tag{41a}$$

$$q_2(t) = a_2 \cos\left(\frac{\Omega}{2}t - \frac{\gamma_2 + \gamma_3}{2}\right), \tag{41b}$$

$$q_3(t) = a_3 \cos(\Omega t - \gamma_3), \tag{41c}$$

where a_i and γ_i take the values of a particular stable fixed point. Thus, γ_3 is the phase difference between directly excited mode q_3 and excitation, and γ_1 and γ_2 are the phase differences between modes excited through internal resonance on the one hand—respectively q_1 and q_2—and q_3 on the other hand.

6. Conclusion

In this paper, a detailed analysis of the non-linear vibrations of thin shallow spherical shells with a free edge has been proposed. The validity range of the governing equations has been quantified analytically and by comparison with a numerical solution. Then, a method of resolution via projection onto the linear modes basis has been detailed, hence presenting the general problem including asymmetric vibrations in a uniform manner.

The major set of results is the general non-linear modal interaction rules that have been established, thanks to computation of all coefficients of the non-linear quadratic and cubic terms that appear in the differential equations. Those coefficients are of major interest as their values govern the energy exchanges between mode that are likely to appear at the non-linear stage. It has been shown that an internal resonance relation between the natural frequencies of the shell is not a sufficient condition for the non-linear modal interaction to occur, since some coefficients of the non-linear terms vanish. This is a consequence of the rotational symmetry of the geometry of the structure, and coupling rules that hold on the number of nodal diameters of the involved modes have been derived. It is thus possible to predict if a particular *non-linear* energy exchange between modes is possible by considering only the *linear* modal analysis of the structure: the values of the natural frequencies determine the possible internal resonances and the number of nodal diameters of the involved modes enable to conclude on the activation of the modal interaction. Finally, an application has been treated: the specific case of a 1:1:2 internal resonance has been revisited, with emphasis on the effect of the slight imperfections of the structure on the energy transfers.

Beyond the important results derived throughout this study, the developed model framework can now be used for studying the rich variety of behaviour exhibited by non-linear shell vibrations. As the results of this

article are based on the rotational symmetry of the structure, similar results can be expected for other axisymmetric shells (cylindrical, conical or any profile). An experimental validation of the 1:1:2 internal resonance will be soon reported, showing the validity range and the precision of the model. More generally, this study can serve as a basis for analytical, or numerical-analytical solutions, computations of non-linear normal modes for prediction of the trend of non-linearity, or, in a different point of view, for analysis and synthesis of the sound produced by musical instruments such as cymbals and gongs (Chaigne et al., 2004).

Acknowledgement

The authors want to thank Éric Luminais for the scrupulous reading of the manuscript he has made.

Appendix A. Expression of the eigenmodes of the shell

This section is based on the work of Johnson and Reissner (1956), to which the interested reader can refer for further details.

A.1. General case

The eigenmodes are solutions of the linear, undamped and homogeneous problem related to Eqs. (11a) and (11b), that is written

$$\Delta\Delta w + \varepsilon_q \Delta F + \ddot{w} = 0, \tag{A.1a}$$

$$\Delta\Delta F = \frac{a^4}{Rh^3}\Delta w. \tag{A.1b}$$

The solution is separated in space and time by

$$w(r,\theta,t) = \Phi(r,\theta)q(t) \quad \text{and} \quad F(r,\theta,t) = \frac{a^4}{Rh^3}\Psi(r,\theta)q(t), \tag{A.2}$$

where w and F have the same time dependence because F is slaved to w by Eq. (A.1b). Thus, Φ and Ψ are solutions of

$$\Delta\Delta\Phi + \chi\Delta\Psi - \omega^2\Phi = 0 \quad \text{and} \quad \Delta\Delta\Psi = \Delta\Phi. \tag{A.3}$$

Eq. (A.3) writes

$$\Delta[\Delta\Delta + \chi - \omega^2]\Phi = 0, \tag{A.4}$$

where curvature parameter χ is defined by Eq. (8a). Two cases must now be considered.

- *Case I: modes written in terms of Bessel functions*

$$\omega^2 = \chi + \zeta^4, \quad \Delta[\Delta\Delta - \zeta^4]\Phi(r,\theta) = 0, \tag{A.5}$$

$$\Phi_{kn}(r,\theta) = \underbrace{\kappa_{kn}\left[A_k(\zeta_{kn})r^k + J_k(\zeta_{kn}r) + C_k(\zeta_{kn})I_k(\zeta_{kn}r)\right]}_{R_{kn}(r)} \left| \begin{matrix}\cos k\theta \\ \sin k\theta\end{matrix}\right., \tag{A.6}$$

$$\Psi_{kn}(r,\theta)=\kappa_{kn}\left[D_k(\zeta_{kn})r^k+\left(1+\frac{\zeta_{kn}^4}{\chi}\right)\frac{A_k(\zeta_{kn})}{4(k+1)}r^{k+2}-\frac{1}{\zeta_{kn}^2}\left(J_k(\zeta_{kn}r)-C_k(\zeta_{kn})I_k(\zeta_{kn}r)\right)\right]\left|\begin{matrix}\cos k\theta\\ \sin k\theta\end{matrix}\right.. \tag{A.7}$$

- *Case II: modes written in terms of Kelvin functions*

$$\zeta^4<\chi,\quad \omega^2=\chi-\zeta^4,\quad \Delta\left[\Delta\Delta+\zeta^4\right]\Phi(r,\theta)=0, \tag{A.8}$$

$$\Phi_{kn}(r,\theta)=\underbrace{\kappa_{kn}\left[A_k(\zeta_{kn})r^k+\mathrm{ber}_k(\zeta_{kn}r)+C_k(\zeta_{kn})\mathrm{bei}_k(\zeta_{kn}r)\right]}_{R_{kn}(r)}\left|\begin{matrix}\cos k\theta\\ \sin k\theta\end{matrix}\right., \tag{A.9}$$

$$\Psi_{kn}(r,\theta)=\kappa_{kn}\left[D_k(\zeta_{kn})r^k+\left(1-\frac{\zeta_{kn}^4}{\chi}\right)\frac{A_k(\zeta_{kn})}{4(k+1)}r^{k+2}+\frac{1}{\zeta_{kn}^2}\left(\mathrm{bei}_k(\zeta_{kn}r)-C_k(\zeta_{kn})\mathrm{ber}_k(\zeta_{kn}r)\right)\right]\left|\begin{matrix}\cos k\theta\\ \sin k\theta\end{matrix}\right.. \tag{A.10}$$

In the above equations, A_k, C_k and D_k are constants depending on boundary conditions, κ_{kn} is a normalization constant, k is the number of nodal diameters and n the number of nodal circles. J_k denotes the Bessel function of the first kind of order k and $I_k(x)=J_k(\mathrm{i}x)$ with $\mathrm{i}=\sqrt{-1}$. Kelvin functions are defined by $\mathrm{ber}_k(x)+\mathrm{i}\,\mathrm{bei}_k(x)=J_k(\mathrm{i}^{3/2}x)=(-1)^kI_k(i^{1/2}x)$. The normalization constant κ_{kn} is chosen so that Eq. (22) is fulfilled. Modes Ψ_{kn} are not normalized (κ_{kn} appears in Φ_{kn} as well as in Ψ_{kn}) as they are slaved to transverse modes Φ_{kn}.

A.2. Free-edge boundary conditions

Values of ζ, A_k, C_k and D_k are determined by introducing the boundary conditions. In the case of a free-edge, one obtains in a dimensionless form (see Eqs. (5a)–(5d)):

$$\Phi \quad\text{and}\quad \Psi \text{ are bounded at } r=0, \tag{A.11a}$$

$$\Phi_{,rr}+\nu\Phi_{,r}+\nu\Phi_{,\theta\theta}=0 \quad \text{at } r=1, \tag{A.11b}$$

$$\Phi_{,rrr}+\Phi_{,rr}-\Phi_{,r}+(2-\nu)\Phi_{,r\theta\theta}-(3-\nu)\Phi_{,\theta\theta}=0 \quad \text{at } r=1, \tag{A.11c}$$

$$\Psi_{,r}+\Psi_{,\theta\theta}=0,\quad \Psi_{,r\theta}-\Psi_{,\theta}=0 \quad \text{at } r=1. \tag{A.11d}$$

The expressions of the modes in terms of Bessel functions or Kelvin functions depends on the values of k, n and χ, results that are summarized in Table A.3.

- *Axisymmetric modes and modes with one nodal diameter* ($k\in\{0,1\}$)
  The modes express in terms of Bessel functions, so that $\zeta_{kn}=\zeta_{kn}^{(0)}$ is the nth zero of the equation

$$\mathscr{D}_k(\zeta)=0 \tag{A.12}$$

with $\mathscr{D}_k$ defined in Table A.1. This equation is independent of χ—and then of curvature—and is the equation with whom are calculated the natural frequencies (denoted by $\omega_{kn}^{(0)}=\zeta_{kn}^{(0)2}$) of the circular plate obtained with $\chi=0$. The natural frequencies of the shell are then, from Eq. (A.5), for all $k\in\{0,1\}$ and for all n

$$\omega_{kn}=\sqrt{\chi+\zeta_{kn}^4}=\sqrt{\chi+\omega_{kn}^{(0)2}}. \tag{A.13}$$

Table A.1
Coefficients for modes in terms of Bessel function

$M_{33} = \zeta(\nu-1)J'_k(\zeta) + [k^2(1-\nu) - \zeta^2]J_k(\zeta),$
$M_{34} = \zeta(\nu-1)I'_k(\zeta) + [k^2(1-\nu) + \zeta^2]I_k(\zeta),$
$M_{43} = \zeta[k^2(\nu-1) - \zeta^2]J'_k(\zeta) + k^2(1-\nu)J_k(\zeta),$
$M_{44} = \zeta[k^2(\nu-1) + \zeta^2]I'_k(\zeta) + k^2(1-\nu)I_k(\zeta),$
$\mathscr{D}_k(\zeta) = M_{33}M_{43} - M_{34}M_{44}.$
$\tilde{J}_k(\zeta) = kM_{33} + M_{43}, \tilde{I}_k(\zeta) = kM_{34} + M_{44},$
$C_k(\zeta) = -\frac{\tilde{J}_k(\zeta)}{\tilde{I}_k(\zeta)},$
$A_k(\zeta) = -\frac{2(1+k)\chi}{\zeta^2(\chi+\zeta^4)}\left[C_k(\zeta)(kI_k(\zeta) - \zeta I'_k(\zeta)) + (kJ_k(\zeta) - \zeta J'_k(\zeta))\right],$
$D_k(\zeta) = \frac{1}{2\zeta^2}\left[C_k(\zeta)((k+2)I_k(\zeta) - \zeta I'_k(\zeta)) + ((k+2)J_k(\zeta) - \zeta J'_k(\zeta))\right],$

The mode shapes are obtained by Eqs. (A.6), (A.7) and coefficients of Table A.1. One can show that $A_0 = A_1 = 0$. As a consequence, for all $k \in \{0,1\}$, both transverse and membrane mode shapes do not depend on curvature and transverse modes Φ_{kn} are identical to those of the corresponding plate (see e.g. Touzé et al., 2002). Thus, for all $k \in \{0,1\}$ and for all n

$$\Phi_{kn}(r,\theta) = \kappa_{kn}\left(J_k(\zeta_{kn}r) - \frac{\tilde{J}_k(\zeta_{kn})}{\tilde{I}_k(\zeta_{kn})}I_k(\zeta_{kn}r)\right)\begin{vmatrix}\cos k\theta\\ \sin k\theta\end{vmatrix} \tag{A.14}$$

with $\tilde{J}_k(\zeta)$ and $\tilde{I}_k(\zeta)$ defined in Table A.1.

- *Asymmetric modes with* $k \geqslant 2$
  The particular value of χ defined by

$$\chi_k^{lim} = \frac{(1-\nu)(3+\nu)k^2(k^2-1)}{1 + \frac{1}{4}(1-\nu)(k-2) - \frac{k^2(k-1)(1-\nu)(4k-\nu+9)}{16(k+2)^2(k+3)}} \tag{A.15}$$

determines whether the modes writes in terms of Kelvin functions or Bessel functions.

  – If $\chi < \chi_k^{lim}$, all modes are written in term of Bessel functions. ζ_{kn} is the $(n+1)$th zero of the equation

$$\frac{\zeta^4}{\chi} = \frac{\mathscr{S}_k(\zeta)}{\mathscr{R}_k(\zeta)} - 1 \quad \text{and} \quad \omega_{kn} = \sqrt{\chi + \zeta_{kn}^4}. \tag{A.16}$$

In the above equations,

$$\mathscr{S}_k(\zeta) = \frac{k}{\zeta}(\nu-1)(k-1)\left[\tilde{J}_k(\zeta)\left(\frac{k}{\zeta}I_k(\zeta) - I'_k(\zeta)\right) + \tilde{I}_k(\zeta)\left(\frac{k}{\zeta}J_k(\zeta) - J'_k(\zeta)\right)\right], \tag{A.17}$$

$$\mathscr{R}_k(\zeta) = -\frac{1}{2(1+k)}\mathscr{D}_k(\zeta), \tag{A.18}$$

with $\tilde{J}_k(\zeta)$, $\tilde{I}_k(\zeta)$ and $\mathscr{D}_k(\zeta)$ defined in Table A.1. The mode shapes are obtained by Eqs. (A.6) and (A.7) and coefficients of Table A.1.

  – If $\chi > \chi_k^{lim}$, modes with no nodal circles ($n = 0$) writes in term of Kelvin functions and the others in terms of Bessel functions. Thus, ζ_{k0} is the only zero of equation:

$$\frac{\zeta^4}{\chi} = 1 - \frac{\mathscr{U}_k(\zeta)}{\mathscr{T}_k(\zeta)} \quad \text{and} \quad \omega_{k0} = \sqrt{\chi - \zeta_{k0}^4}. \tag{A.19}$$

Table A.2
Coefficients for modes in terms of Kelvin function

$M_{33} = \zeta^2 \mathrm{ber}_k''(\zeta) + v\zeta \mathrm{ber}_k'(\zeta) - k^2 v \mathrm{ber}_k(\zeta)$
$M_{34} = \zeta^2 \mathrm{bei}_k''(\zeta) + v\zeta \mathrm{bei}_k'(\zeta) - k^2 v \mathrm{bei}_k(\zeta)$
$M_{43} = \zeta^3 \mathrm{ber}_k'''(\zeta) + \zeta^2 \mathrm{ber}_k''(\zeta) - \zeta[1 + k^2(2 - v)]\mathrm{ber}_k'(\zeta) + k^2(3 - v)\mathrm{ber}_k(\zeta)$
$M_{44} = \zeta^3 \mathrm{bei}_k'''(\zeta) + \zeta^2 \mathrm{bei}_k''(\zeta) - \zeta[1 + k^2(2 - v)]\mathrm{bei}_k'(\zeta) + k^2(3 - v)\mathrm{bei}_k(\zeta)$
$\mathscr{D}_k(\zeta) = M_{33}M_{43} - M_{34}M_{44}$
$\tilde{J}_k(\zeta) = kM_{33} + M_{43}, \tilde{I}_k(\zeta) = kM_{34} + M_{44}$
$C_k(\zeta) = -\frac{\tilde{J}_k(\zeta)}{\tilde{I}_k(\zeta)},$
$A_k(\zeta) = \frac{2(1+k)\chi}{\zeta^2(\chi - \zeta^4)}[C_k(\zeta)(k\mathrm{ber}_k(\zeta) - \zeta \mathrm{ber}_k'(\zeta)) + (k\mathrm{bei}_k(\zeta) - \zeta \mathrm{bei}_k'(\zeta))]$
$D_k(\zeta) = -\frac{1}{2\zeta^2}[C_k(\zeta)((k+2)\mathrm{ber}_k(\zeta) - \zeta \mathrm{ber}_k'(\zeta)) + ((k+2)\mathrm{bei}_k(\zeta) - \zeta \mathrm{bei}_k'(\zeta))]$

Table A.3
Summary of calculation of modes of a spherical shell

$k \in \{0, 1\}$	$\forall n \geqslant 1$	"Bessel" $\omega_{kn} = \sqrt{\chi + \omega_{kn}^{(0)2}}$ Eqs. (A.7), (A.12) and (A.14), Table A.1	
$k \geqslant 2$	$n = 0$	$\chi < \chi_k^{lim}$	$\chi > \chi_k^{lim}$
		"Bessel" $\omega_{k0} = \sqrt{\chi + \zeta_{k0}^4}$ Eqs. (A.6), (A.7) and (A.16) Table A.1	"Kelvin" $\omega_{k0} = \sqrt{\chi - \zeta_{k0}^4}$ Eqs. (A.9), (A.10), (A.19), Table A.2
$k \geqslant 2$	$n \geqslant 1$	"Bessel" $\omega_{kn} = \sqrt{\chi + \zeta_{kn}^4}$ Eqs. (A.6), (A.7) and (A.16), Table A.1	

$\omega_{kn}^{(0)}$ are the frequencies of the corresponding circular plate and χ_k^{lim} is defined by Eq. (A.15).

In the above equation

$$\mathscr{U}_k(\zeta) = -\frac{k}{\zeta}(v-1)(k-1)\left[\tilde{J}_k(\zeta)\left(\frac{k}{\zeta}\mathrm{ber}_k(\zeta) - \mathrm{ber}_k'(\zeta)\right) + \tilde{I}_k(\zeta)\left(\frac{k}{\zeta}\mathrm{bei}_k(\zeta) - \mathrm{bei}_k'(\zeta)\right)\right] \tag{A.20}$$

$$\mathscr{T}_k(\zeta) = -\frac{1}{2(1+k)}\mathscr{D}_k(\zeta) \tag{A.21}$$

and $\tilde{J}_k(\zeta)$, $\tilde{I}_k(\zeta)$ and $\mathscr{D}_k(\zeta)$ are defined in Table A.2. The corresponding mode shapes are obtained by Eq. (A.9) and (A.10) and coefficients of Table A.2. For modes with at least one nodal circle ($n \geqslant 1$), ζ_{kn} is the nth zero of Eq. (A.16), ω_{kn} is defined by Eq. (A.16) and the corresponding mode shapes writes with Eqs. (A.6) and (A.7) and coefficients of Table A.1.

Appendix B. Expression of functions Υ_b

Functions $\Upsilon_b(r, \theta)$ are solutions of

$$(\Delta\Delta - \xi^4)\Upsilon = 0, \tag{B.1a}$$

$$\Upsilon = 0 \quad \text{at } r = 1 \tag{B.1b}$$

$$\Upsilon_{,r} = 0 \quad \text{at } r = 1, \tag{B.1c}$$

$$\Upsilon \text{ is bounded in } r = 0. \tag{B.1d}$$

One obtains

$$\Upsilon_{lm}(r,\theta) = \lambda_{lm}\left[J_l(\xi_{lm}r) - \frac{J_l(\xi_{lm})}{I_l(\xi_{lm})} I_l(\xi_{lm}r)\right] \left| \begin{matrix} \cos l\theta \\ \sin l\theta \end{matrix} \right. \tag{B.2}$$

where the ξ_{lm} is the mth solution of the following equation:

$$J_{l-1}(\xi) I_l(\xi) - I_{l-1}(\xi) J_l(\xi) = 0. \tag{B.3}$$

Computed values of the ξ_{lm} can be found in Leissa (1993a). The normalization constant λ_{lm} is chosen so that Eq. (17) is fulfilled.

Appendix C. Calculation of coupling coefficients β^s_{pq} and Υ^s_{pqu}

The different modes that are necessary for the calculation of coefficients β^s_{pq} and Γ^s_{pqu} (Eqs. (20) and (21)) are noted separated in r and θ

$$\Phi_{0n}(r) = R_{0n}(r) \quad \text{for } k = 0; \quad \left.\begin{matrix} \Phi_{kn1}(r,\theta) \\ \Phi_{kn2}(r,\theta) \end{matrix}\right| = R_{kn}(r) \left| \begin{matrix} \cos k\theta \\ \sin k\theta \end{matrix} \right. \quad \text{for } k \geqslant 1;$$

$$\Psi_{0n}(r) = S_{0n}(r) \quad \text{for } k = 0; \quad \left.\begin{matrix} \Psi_{kn1}(r,\theta) \\ \Psi_{kn2}(r,\theta) \end{matrix}\right| = S_{kn}(r) \left| \begin{matrix} \cos k\theta \\ \sin k\theta \end{matrix} \right. \quad \text{for } k \geqslant 1;$$

$$\Upsilon_{0m}(r) = T_{0m}(r) \quad \text{for } l = 0; \quad \left.\begin{matrix} \Upsilon_{lm1}(r,\theta) \\ \Upsilon_{lm2}(r,\theta) \end{matrix}\right| = T_{lm}(r) \left| \begin{matrix} \cos l\theta \\ \sin l\theta \end{matrix} \right. \quad \text{for } l \geqslant 1.$$

In the following, subscripts γ and δ will denote the nature in cosine ($\gamma = 1$) or sine ($\gamma = 2$) of the considered mode. In order to lighten notations, subscripts p, q, s and b will sometimes replace triplets (k_p, n_p, γ_p) to identify modes Φ, Ψ and Υ. For example, Φ_p is the same than $\Phi_{k_p n_p \gamma_p}$, so that $\Phi_p(r,\theta) = R_{k_p n_p}(r)\cos k_p\theta$ if $\gamma_p = 1$ and $\Phi_p(r,\theta) = R_{k_p n_p}(r)\sin k_p\theta$ if $\gamma_p = 2$. In the same manner, $R_p(r) = R_{k_p n_p}(r)$.

C.1. Quadratic coefficients β^s_{pq}

Their expression is (Eq. (20)):

$$\beta^s_{pq} = -\underbrace{\iint_{\mathscr{S}_\perp} \Phi_s L(\Phi_p, \Psi_q)\mathrm{d}S}_{\mathscr{J}^\Psi(s,p,q)} - \frac{1}{2}\sum_{b=1}^{+\infty} \frac{1}{\xi_b^4} \underbrace{\iint_{\mathscr{S}_\perp} L(\Phi_p, \Phi_q)\Upsilon_b \,\mathrm{d}S}_{\mathscr{I}(p,q,b)} \underbrace{\iint_{\mathscr{S}_\perp} \Phi_s \Delta\Upsilon_b \mathrm{d}S}_{\mathscr{K}(s,b)}. \tag{C.1}$$

Following the definition of L (Eq. (4)) and integrating over domain $\mathscr{S}_\perp$ by separation of variables r and θ, one obtains

$$\mathscr{I}(p,q,b) = \mathbf{I}_1(p,q,b)\mathbf{\Pi}^{(1)}_{\gamma_p\gamma_q\delta}(k_p,k_q,l) - 2k_pk_q\mathbf{I}_2(p,q,b)\mathbf{\Pi}^{(2)}_{\gamma_p\gamma_q\delta}(k_p,k_q,l), \tag{C.2}$$

$$\mathscr{J}^{\Psi}(s,p,q) = \mathbf{J}_1^{\Psi}(s,p,q)\mathbf{\Pi}^{(1)}_{\gamma_s\gamma_p\gamma_q}(k_s,k_p,k_q) - 2k_pk_q\mathbf{J}_2^{\Psi}(s,p,q)\mathbf{\Pi}^{(3)}_{\gamma_s\gamma_p\gamma_q}(k_s,k_p,k_q), \tag{C.3}$$

$$\mathscr{K}(s,b) = \mathbf{K}(s,b)\mathbf{\Pi}^{(4)}_{\gamma_s\delta}(s,b), \tag{C.4}$$

where

$$\mathbf{I}_1(p,q,b) = \int_0^1 \left[R_p''\left(R_q' - k_q^2\frac{R_q}{r}\right) + R_q''\left(R_p' - k_p^2\frac{R_p}{r}\right)\right]T_b\mathrm{d}r, \tag{C.5}$$

$$\mathbf{I}_2(p,q,b) = \int_0^1 \frac{1}{r}\left[R_p' - \frac{R_p}{r}\right]\left[R_q' - \frac{R_q}{r}\right]T_b\mathrm{d}r, \tag{C.6}$$

$$\mathbf{J}_1^{\Psi}(s,p,q) = \int_0^1 R_s\left[R_p''\left(S_q' - k_q^2\frac{S_q}{r}\right) + S_q''\left(R_p' - k_p^2\frac{R_p}{r}\right)\right]\mathrm{d}r, \tag{C.7}$$

$$\mathbf{J}_2^{\Psi}(s,p,q) = \int_0^1 R_s\frac{1}{r}\left[R_p' - \frac{R_p}{r}\right]\left[S_q' - \frac{S_q}{r}\right]\mathrm{d}r, \tag{C.8}$$

$$\mathbf{K}(s,b) = \int_0^1 R_s\left(rT_b'' + T_b' - l^2\frac{T_b}{r}\right)\mathrm{d}r \tag{C.9}$$

and

$$\mathbf{\Pi}^{(1)}_{\gamma\gamma'\delta}(k,k',l) = \int_0^{2\pi}\begin{vmatrix}\cos k\theta & \cos k'\theta & \cos l\theta\\ \cdot & \cdot & \cdot\\ \sin k\theta & \sin k'\theta & \sin l\theta\end{vmatrix}\mathrm{d}\theta,$$

$$\mathbf{\Pi}^{(2)}_{\gamma\gamma'\delta}(k,k',l) = \int_0^{2\pi}\begin{vmatrix}-\sin k\theta & -\sin k'\theta & \cos l\theta\\ \cdot & \cdot & \cdot\\ \cos k\theta & \cos k'\theta & \sin l\theta\end{vmatrix}\mathrm{d}\theta,$$

$$\mathbf{\Pi}^{(3)}_{\gamma\gamma'\delta}(k,k',l) = \int_0^{2\pi}\begin{vmatrix}\cos k\theta & -\sin k'\theta & -\sin l\theta\\ \cdot & \cdot & \cdot\\ \sin k\theta & \cos k'\theta & \cos l\theta\end{vmatrix}\mathrm{d}\theta,$$

$$\mathbf{\Pi}^{(4)}_{\gamma\delta}(k,l) = \int_0^{2\pi}\begin{vmatrix}\cos k\theta & \cos l\theta\\ \cdot & \cdot\\ \sin k\theta & \sin l\theta\end{vmatrix}\mathrm{d}\theta.$$

The above notations mean that any $\mathbf{\Pi}_{\gamma\gamma'\delta}$ is obtained by making the product of three functions sine and/or cosine, each one being taken in a column of the above matrices. (γ,γ',δ) refers, respectively, to the first, the second and the third column and their values determine the line. For example, with $(\gamma,\gamma',\delta) = (2,1,2)$

$$\mathbf{\Pi}^{(3)}_{212}(k,k',l) = -\int_0^{2\pi}\sin k\theta\sin k'\theta\cos l\theta\mathrm{d}\theta.$$

Several coefficients $\mathbf{\Pi}$ equal zero for specific values of (k,k',l) (the numbers of nodal diameters) and (γ,γ',δ) (the nature in sine and/or cosine). This is the cause of the vanishing of some coefficients β^s_{pq}. The results on

Table C.1
Conditions on modes Φ_p, Φ_q, Φ_s and Υ_b that lead to non-zero $\mathscr{I}(p,q,b)$, $\mathscr{K}(s,b)$ and $\mathscr{J}^{\Psi}(s,p,q)$

$\mathscr{J}^{\Psi}(s,p,q)\neq 0$ $\Downarrow$ $k_s\in\{k_p+k_q,\lvert k_p-k_q\rvert\}$			$\mathscr{I}(p,q,b)\neq 0$ $\Downarrow$ $l\in\{k_p+k_q,\lvert k_p-k_q\rvert\}$			$\mathscr{K}(s,b)\neq 0$ $\Downarrow$ $l=k_s$	
Φ_s,γ_s	Φ_p,γ_p	$\Phi_q,\gamma_q,\Psi_q,\gamma_q$	Φ_p,γ_p	Φ_q,γ_q	Υ_b,δ	Φ_s,γ_s	Υ_b,δ
cos, 1	cos, 1	cos, 1	cos, 1	cos, 1	cos, 1	cos, 1	cos, 1
	sin, 2	sin, 2	sin, 2	sin, 2		sin, 2	sin, 2
sin, 2	cos, 1	sin, 2	sin, 2	cos, 1	sin, 2		
	sin, 2	cos, 1	cos, 1	sin, 2			

$\mathscr{I}(p,q,b)$, $\mathscr{K}(s,b)$ and $\mathscr{J}^{\Psi}(s,p,q)$ are summarized in Table C.1. To obtain a non-zero β^s_{pq}, one must have either $\mathscr{J}^{\Psi}(s,p,q)\neq 0$ or at least one mode Υ_b so that $\mathscr{I}(p,q,b)\mathscr{K}(s,b)\neq 0$. It is summarized in Table 2.

C.2. Cubic coefficients Γ^s_{pqu}

Their expression is (Eq. (20)):

$$\Gamma^s_{pqu}=\frac{1}{2}\sum_{b=1}^{+\infty}\frac{1}{\xi_b^4}\underbrace{\int\int_{\mathscr{S}}L(\Phi_p,\Phi_q)\Upsilon_b\mathrm{d}S}_{\mathscr{I}(p,q,b)}\underbrace{\int\int_{\mathscr{S}}\Phi_sL(\Phi_u,\Upsilon_b)\mathrm{d}S}_{\mathscr{J}^{\Upsilon}(s,u,b)},\tag{C.10}$$

where $\mathscr{I}(p,q,b)$ has been calculated in the above section and $\mathscr{J}^{\Upsilon}(s,u,b)$ has the same structure than $\mathscr{J}^{\Psi}(s,p,q)$ and writes

$$\mathscr{J}^{\Upsilon}(s,u,b)=\mathbf{J}_1^{\Upsilon}(s,u,b)\mathbf{\Pi}^{(1)}_{\gamma_s,\gamma_u,\delta}(k_s,k_u,l)-2k_ul\mathbf{J}_2^{\Upsilon}(s,u,b)\mathbf{\Pi}^{(3)}_{\gamma_s,\gamma_u,\delta}(k_s,k_u,l),\tag{C.11}$$

where

$$\mathbf{J}_1^{\Upsilon}(s,u,b)=\int_0^1R_s\left[R_u''\left(T_b''-l^2\frac{T_b}{r}\right)+T_b''\left(R_u'-k_u^2\frac{R_u}{r}\right)\right]\mathrm{d}r,\tag{C.12}$$

$$\mathbf{J}_2^{\Upsilon}(s,s,b)=\int_0^1R_s\frac{1}{r}\left[R_u'-\frac{R_u}{r}\right]\left[T_b'-\frac{T_b}{r}\right]\mathrm{d}r.\tag{C.13}$$

Again, non-zero Γ^s_{pqu} are obtained if $\mathscr{I}(p,q,b)\mathscr{J}^{\Upsilon}(s,u,b)\neq 0$, cases specified in Table C.2. The consequences on Γ^s_{pqu} are summarized in Table 2.

Table C.2
Conditions on modes Φ_p, Φ_q, Φ_s, Φ_u and Υ_b that lead to non-zero $\mathscr{I}(p,q,b)$ and $\mathscr{J}^{\Upsilon}(s,p,q)$

$\mathscr{I}(p,q,b)\neq 0$ $\Downarrow$ $l\in\{k_p+k_q,\lvert k_p-k_q\rvert\}$			$\mathscr{J}^{\Upsilon}(s,u,b)\neq 0$ $\Downarrow$ $l\in\{k_s+k_u,\lvert k_s-k_u\rvert\}$		
Φ_p,γ_p	Φ_q,γ_q	Υ_b,δ	Φ_s,γ_s	Φ_u,γ_u	Υ_b,δ
cos, 1	cos, 1	cos, 1	cos, 1	cos, 1	cos, 1
sin, 2	sin, 2		sin, 2	sin, 2	
sin, 2	cos, 1	sin, 2	sin, 2	cos, 1	sin, 2
cos, 1	sin, 2		cos,1	sin, 2	

References

Alhazza, K.A., 2002. Nonlinear vibrations of doubly curved cross-ply shallow shells. Ph.D. Thesis, Virginia Polytechnic Institute and State University.

Amabili, M., Païdoussis, M.P., 2003. Review of studies on geometrically nonlinear vibrations and dynamics of circular cylindrical shells and panels, with and without fluid–structure interaction. ASME Appl. Mech. Rev. 56 (4), 349–381.

Amabili, M., Pellicano, R., Païdoussis, M.P., 1998. Nonlinear vibrations of simply supported circular cylindrical shells, coupled to quiescent fluid. J. Fluids Struct. 12, 883–918.

Amabili, M., Pellicano, F., Païdoussis, M.P., 1999. Non-linear dynamics and stability of circular cylindrical shells containing flowing fluid, part II: large-amplitude vibrations without flow. J. Sound Vib. 228 (5), 1103–1124.

Amabili, M., Pellicano, F., Vakakis, A.F., 2000. Nonlinear vibrations and multiple resonances of fluid-filled, circular shells, part 1: equations of motion and numerical results. ASME J. Vib. Acoust. 122, 346–354.

Benedettini, F., Rega, G., Alaggio, R., 1995. Non-linear oscillations of a four-degree-of-freedom model of a suspended cable under multiple internal resonance conditions. J. Sound Vib. 182 (5), 775–798.

Chaigne, A., Touzé, C., Thomas, O., 2004. Mechanical models of musical instruments and sound synthesis: the case of gongs and cymbals. In: Proceedings of the International Symposium on Musical Acoustics. Nara, Japan.

Chin, C.-M., Nayfeh, A.H., 2001. A second-order approximation of multi-modal interactions in externally excited circular cylindrical shells. Nonlinear Dynam. 26, 45–66.

Chu, H.-N., Herrmann, G., 1956. Influence of large amplitudes on free flexural vibrations of rectangular elastic plates. J. Appl. Mech. 23, 532–540.

Donnell, L.H., 1934. A new theory for the buckling of thin cylinders under axial compression and bending. Trans. Am. Soc. Mech. Eng. 56, 795–806.

Efstathiades, G.J., 1971. A new approach to the large-deflction vibrations of imperfect circular disks using Galerkin's procedure. J. Sound Vib. 16 (2), 231–253.

Evensen, D.A., Fulton, R.E., oct 1965. Some studies on the nonlinear dynamic response of shell-type structures. Tech. Rep. TMX 56843, NASA Langley Research Center.

Evensen, H.A., Evan-Iwanowsky, R.M., 1967. Dynamic response and stability of shallow spherical shells subject to time-dependant loading. AIAA J. 5 (5), 969–976.

Gonçalves, P.B., 1994. Axisymmetric vibrations of imperfect shallow spherical caps under pressure loading. J. Sound Vib. 174 (2), 249–260.

Grossman, P.L., Koplik, B., Yu, Y.-Y., 1969. Nonlinear vibrations of shallow spherical shells. ASME J. Appl. Mech 39E, 451–458.

Guckenheimer, J., Holmes, P., 1983. Nonlinear Oscillations, Dynamical Systems and Bifurcations of Vector Fields. Springer-Verlag, New York.

Guckenheimer, J., Myers, M., Wicklin, F., Worfolk, P., 1995. Dstool: a dynamical system toolkit with an interactive graphical interface. Technical Report, Center for Applied Mathematics, Cornell University.

Haddow, A.G., Barr, A.D.S., Mook, D.T., 1984. Theoretical and experimental study of modal interaction in a two-degree-of-freedom structure. J. Sound Vib. 97, 451–473.

Hamdouni, A., Millet, O., 2003. Classification of thin shell models deduced from the nonlinear three-dimensional elasticity, part I: the shallow shells. Arch. Mech. 55 (2), 135–175.

Hui, D., 1983. Large-amplitude vibrations of geometrically imperfect shallow spherical shells with structural damping. AIAA J. 21 (12), 1736–1741.

Johnson, M.W., Reissner, E., 1956. On transverse vibrations of shallow spherical shells. Quart. Appl. Math. 15 (4), 367–380.

Kalnins, A., 1964. Effect of bending on vibrations of spherical shells. J. Acoust. Soc. Am. 36 (1), 74–81.

Koiter, W.T., 1965. On the nonlinear theory of thin elastic shells, part I, II and III. Proc. Kon. Neth. Akad. Wet. B69, 1–54.

Lacarbonara, W., Rega, G., Nayfeh, A.H., 2003. Resonant non-linear normal modes, part I: analytical treatment for structural one-dimensional systems. Int. J. Non-Linear Mech. 38, 851–872.

Lee, W.K., Yeo, M.H., Samoilenko, S.B., 2003. The effect of the number of nodal diameters on non-linear interactions in two asymmetric vibration modes of a circular plate. J. Sound. Vib 268 (5), 1013–1023.

Leissa, A.W., 1993a. Vibration of plates. Acoustical Society of America (original issued NASA SP-160, 1969).

Leissa, A.W., 1993b. Vibration of shells. Acoustical Society of America (original issued NASA SP-288, 1973).

Leissa, A.W., Kadi, A.S., 1971. Curvature effects on shallow shell vibrations. J. Sound. Vib. 16 (2), 173–187.

Lobitz, D.W., Nayfeh, A.H., Mook, D.T., 1977. Non-linear analysis of vibrations of irregular plates. J. Sound. Vib. 50 (2), 203–217.

Marguerre, K., 1938. Zur Theorie der Gekrümmten Platte Grosser Formänderung. In: Proceedings of the 5th International Congress on Applied Mechanics, pp. 93–101.

Miles, J.W., 1984. Resonantly forced motion of two quadratically coupled oscillators. Physica D 13, 247–260.

Morand, H.J.-P., Ohayon, R., 1995. Fluid Structure Interaction. John Wiley and Sons, New York.

Moussaoui, F., Benamar, R., 2002. Non-linear vibrations of shell-type structures: a review with bibliography. J. Sound. Vib. 255 (1), 161–184.
Mushtari, K.M., Galimov, K.Z., 1961. Non-linear theory of thin elastic shells. Israel Program for Scientific Translations (Russian ed., 1957).
Nayfeh, A.H., 2000. Nonlinear interactions: analytical, computational and experimental methods. In: Wiley Series in Nonlinear Science, New York.
Nayfeh, A.H., Balachandran, B., 1989. Modal interactions in dynamical and structural systems. ASME Appl. Mech. Rev. 42 (11), 175–201.
Nayfeh, A.H., Mook, D.T., 1979. Nonlinear Oscillations. John Wiley and Sons Inc, New York.
Nayfeh, A.H., Nayfeh, J.F., Mook, D.T., 1992. On methods for continuous systems with quadratic and cubic nonlinearities. Nonlinear Dynam. 3, 145–162.
Nayfeh, A.H., Nayfeh, S.A., 1994. On nonlinear modes of continuous systems. J. Vib. Acoust. 116, 129–136.
Nayfeh, A.H., Raouf, R.A., 1987. Non-linear oscillations of circular cylindrical shells. Int. J. Solids Struct. 23 (12), 1625–1638.
Nayfeh, A.H., Zavodney, L.D., 1988. Experimental observation of amplitude and phase-modulated responses of two internally coupled oscillators to a harmonic excitation. ASME J. Appl. Mech. 55, 706–710.
Pellicano, F., Amabili, M., Vakakis, A.F., 2000. Nonlinear vibrations and multiple resonances of fluid-filled, circular shells, part 2: perturbation analysis. ASME J. Vib. Acoust. 122, 355–364.
Qatu, M.S., 2002. Recent research advances in the dynamic behavior of shells: 1989–2000, part 2: homogeneous shells. ASME Appl. Mech. Rev. 55 (5), 415–434.
Raman, A., Mote Jr., C.D., 2001. Effects of imperfection on the non-linear oscillations of circular plates spinning near critical speed. Int. J. Non-linear Mech. 36, 261–289.
Robie, F.M., Popov, A.A., Thompson, J., 1999. Auto-parametric resonance in cylindrical shells using geometric averaging. J. Sound Vib. 227 (1), 65–84.
Soedel, W., 1981. Vibrations of Shells and Plates. Marcel-Dekker Inc., New York.
Sridhar, S., Mook, D.T., Nayfeh, A.H., 1975. Non-linear resonances in the forced responses of plates, part I: symmetric responses of circular plates. J. Sound Vib. 41 (3), 359–373.
Sridhar, S., Mook, D.T., Nayfeh, A.H., 1978. Non-linear resonances in the forced responses of plates, part II: asymmetric responses of circular plates. J. Sound Vib. 59 (2), 159–170.
Thomas, O., Touzé, C., Chaigne, A., Sep. 2001. Non-linear behavior of gongs through the dynamic of simple rods systems. In: Proceedings of the International Symposium on Musical Acoustics, Perugia, Italy, pp. 173–178.
Tien, W.M., Namachchivaya, N.S., Bajaj, A.K., 1994. Non-linear dynamics of as shallow arch under periodic excitation, I: 1:2 internal resonance. Int. J. Nonlinear Mech. 29 (3), 349–366.
Tobias, S.A., Arnold, R.N., 1957. The influence of dynamical imperfection on the vibration of rotating disks. Proc. of the Instn. of Mech. Eng. 171, 669–690.
Touzé, C., Thomas, O., 2004. Reduced-order modeling for a cantilever beam subjected to harmonic forcing. In: proc. of EUROMECH Colloquium 457: nonlinear modes of vibrating systems. Fréjus, France, pp. 165–168.
Touzé, C., Thomas, O., Chaigne, A., 2002. Asymmetric non-linear forced vibrations of free-edge circular plates, part 1: theory. J. Sound. Vib. 258 (4), 649–676.
Touzé, C., Thomas, O., Chaigne, A., 2004. Hardening/softening behaviour in nonlinear oscillations of structural systems using non-linear normal modes. J. Sound. Vib. 273 (1–2), 77–101.
Verpeaux, P., Charras, T., Millard, A., 1988. Calcul des structures et intelligence artificielle. Pluralis, ed., Paris, http://www-cast3m.cea.fr, Chapter CASTEM 2000: Une approche moderne du calcul des structures.
Yamamoto, T., Yasuda, K., 1977. On the internal resonance in a non-linear two-degree-of-freedom system. Bull. Jpn. Soc. Mech. Eng. 20, 168–175.
Yasuda, K., Kushida, G., 1984. Nonlinear forced oscillations of a shallow spherical shell. Bull. JSME 27 (232), 2233–2240.
Ye, Z.M., 1997. The non-linear vibration and dynamic instability of thin shallow shells. J. Sound Vib. 202 (3), 303–311.
Yeo, M.H., Lee, W.K., 2002. Corrected solvability conditions for non-linear asymmetric vibrations of a circular plate. J. Sound. Vib 257 (4), 653–665.